Volume 5, Number 1, 2011

North University of Baia Mare
Faculty of Engineering
Electrical Engineering Department

Carpathian Journal of Electrical Engineering

NORDTECH PUBLISHER

North University of Baia Mare, Carpathian Journal of Electrical Engineering, Volume 5, Number 1, 2011

ISSN 1843 - 7583

NORTH UNIVERSITY of BAIA MARE
FACULTY of ENGINEERING
ELECTRICAL ENGINEERING DEPARTMENT

RO-430083, Baia Mare, Maramureş county, dr. Victor Babeş street, no. 62A,
phone: +40 (0) 362-401256 **fax:** +40 (0) 262-276153
http://www.ubm.ro

Carpathian Journal of Electrical Engineering

Volume 5, Number 1, 2011
ISSN 1843 – 7583

http://cee.ubm.ro/cjee.html

CONTENTS

ASPECTS REGARDING THE TENSIONS APPEARANCE IN ELECTRIC MACHINES SHAFT

Eleonora **POP,** Gherasim Solovestru **DOMIDE,** Olivian **CHIVER**
North University of Baia Mare
nora@ubm.ro

Key words: machine, electric shaft, voltage, FEM.

Abstract: *The paper deals with the factors that give birth to tensions into the electrical machinery shaft. It will also highlight how each of these factors influences the induced voltage. For conducting the study we used an electromagnetic field calculation program based on the finite element method (FEM).*

1. INTRODUCTION

With an experience of over 40 years, the finite element method is one of the most used methods in the study of electromagnetic fields, but also in other branches of engineering, is the mathematical underpinning of many programs dedicated to numerical calculations of vector fields [1]. The method is easily applicable to complex domains in form, both homogeneous and inhomogeneous, with a relatively simple mathematical apparatus, advantages which have made a world in comparison with the other numerical methods (finite difference method, boundary element method) [1].

1.1 The electromagnetic field equations

The equation that must be resolved by finite element results from laws of electromagnetic field method and it is:

$$\nabla\times\left(\frac{1}{\mu(B)}\nabla\times\overline{A}\right)=\overline{J} \tag{1}$$

By condition $\nabla\overline{A}=0$ equation (1) becomes

$$\Delta\overline{A} = -\mu(B)\overline{J} \tag{2}$$

The magnetic vector potential $\overline{A}$ satisfies in conductor an equation Poisson type and outside these, (when $\overline{J} = 0$), an equation Laplace type. Electric field intensity can be expressed in terms of potential magnetic vector $\overline{A}$ and by the electric scalar V, thus

$$\overline{E} = -\nabla V - \frac{\partial \overline{A}}{\partial t} \tag{3}$$

$$\nabla \times (\frac{1}{\mu(B)} \nabla \times \overline{A}) = -\sigma \nabla V - \sigma \frac{\partial \overline{A}}{\partial t} \tag{4}$$

In the relation (4), the total electric current density is the sum of two components: the first component ($-\sigma\nabla V$) it represents the density due to external sources, that in problems of electromagnetic current discharge in the massive conductive is in itself a unknown, and second ($-\sigma \frac{\partial \overline{A}}{\partial t}$) is the density of the induced currents.

If in the domain of calculation there are conducting bodies moving with speed, $\overline{v}$, the general expression of the conduction current density is,

$$\overline{J} = -\sigma \nabla V - \sigma \frac{\partial \overline{A}}{\partial t} + \sigma \overline{v} \times (\nabla \times \overline{A}) \tag{5}$$

1.2 The boundary conditions

Depending on the border type, boundary conditions can be divided into:

- boundary conditions of calculation domain, which in turn can be of Dirichlet, the Neumann and Robin type;
- Terms of passage, the surfaces of discontinuity for parameters of the analyzed material.

Considering two different environments 1 and 2, separated from the surface S_{12} of the unit vector, the conditions are:

$$\overline{n} \times \left(\overline{H_1} - \overline{H_2}\right)\Big|_{S_{12}} = \overline{J}_S, \tag{6}$$

in the case of a current blade J_s, on the surface $S_{12,}$ If there is no current, then

$$\overline{n} \times \left(\overline{H_1} - \overline{H_2}\right)\Big|_{S_{12}} = 0 \tag{7}$$

$$\overline{n} \cdot \left(\overline{B_1} - \overline{B_2}\right)\Big|S_{12} = 0. \tag{8}$$

In what follows will be specified some of the most important aspects that influence of the results of an analysis by finite element method.

Boundary conditions must be imposed because any analysis assumes a finite domain when in fact, it is infinite. Moving from the real (infinite) to the limited (computational domain boundaries required) a truncation must be made, that the results obtained are close to the real ones. This requires a good knowledge of the subjects which allows a priori estimation of field lines to form borders imposed [1-6].

Another important aspect is geometrically finite element mesh domain and imposing degree polynomial interpolation, because they can describe as accurately analyzed in the field.

As techniques currently used we can mention automatically refining the mesh and increasing polynomial interpolation. Considering the magnetic nonlinearity implies that the value is dependent permeability field values.

The simplest method is to consider the nonlinearity assumed baseline permeability and solve the corresponding linear equations, and then based on the values obtained permeability values are recalculated from the magnetization curves. The cycles are repeated until a difference between two successive values smaller than a prescribed value.

Reducing the computation time required nonlinear harmonic analysis - while important in comparison with a linear harmonic analysis, when all field sizes vary harmonically in time and can therefore be represented in complex derivative discretization is not necessary magnetic vector potential (induced currents corresponding period) - equivalence can be achieved by nonlinear harmonic regime with one linear harmonic. Defining the equivalent magnetization curve $B_e(H_e)$ based on known nonlinear static magnetization curve $B(H)$ is requiring magnetic energy conservation.

2. FEM SIMULATIONS

2.1 The numerical model of the studied machine

Induced electromotive tension can be continuous or alternative depending on the type electric machine. If c.c.machines is specifically induce a continuous voltage in the shaft.As it stands and where synchronous machine. Alternative voltages can occur in all types of electrical machines. The main cause of this is unbalance magnetic circuit which closes magnetic flow useful. The most important values of the voltages are encountered in the case of alternating current machines.

To determine the electromotive tension induced in the shaft of electric machines using finite element method implies the creation of a numerical model corresponding real machine model [2], [3], [4]. Since the voltage induced in the shaft of a rotating machinery is mainly due to the magnetic field in the core of the machine, making a two-dimensional numerical analysis is conservative. Therefore the numerical model necessary will be bidimensional. Numerical analysis type must match the case when electric and magnetic sizes are variable in time, relative to the shaft, which is the situation that leads to induced electromotive tension in it. For this study we considered a three-phase asynchronous motor with six slots per pole and phase two pole pairs and rotor, the corresponding model is shown in *Figure 1.*

The engine power is considerate 500 kW, the inside diameter of the stator is 470 mm, the outside is 740 mm, length 353 mm, and the gap of 1.5 mm. Stator winding up has shortened to 5/6 out of diametrically step, coils corresponding to a phase of the machine can be seen in Figure 2.

As recommended in specialized literature [1] in the case of rotating machines boundary conditions used are those of "tangential flow" of calculation border area is delimited by external armature magnetic of the circuit (stator in the case of normal construction or rotor for cars build in reverse) (*Fig. 3*).

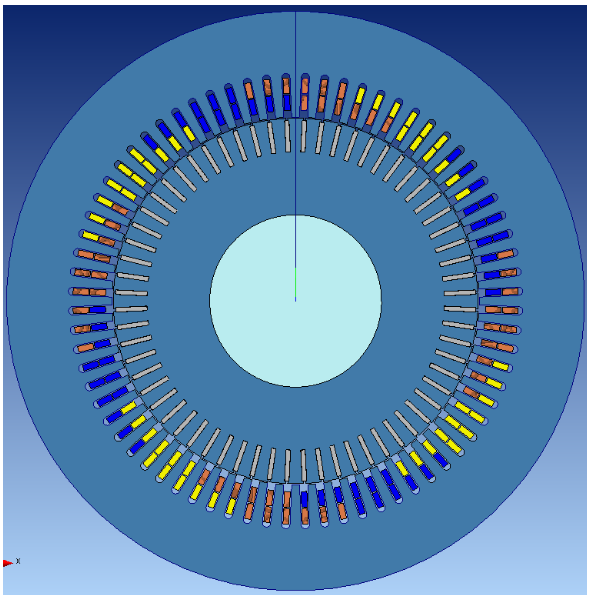

Fig.1. Numeric model

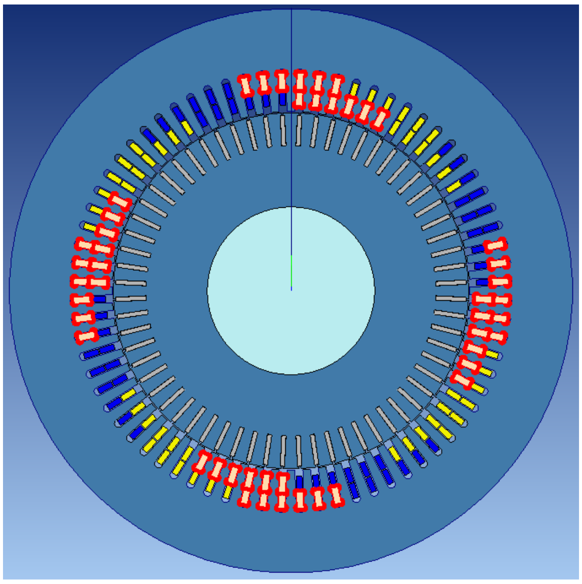

Fig.2. Coils of phase

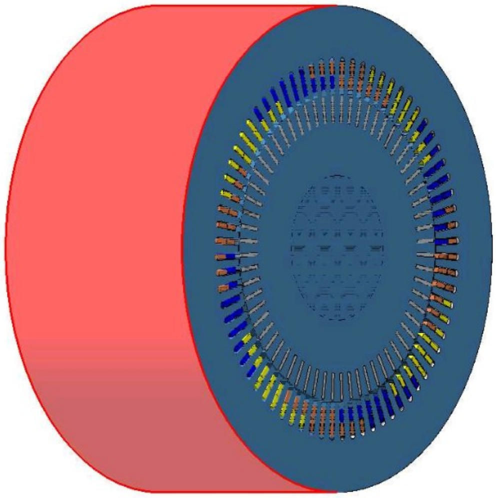

Fig.3. The boundary conditions

` Regarding the conditions under which the analyzes were performed, stated the following: the degree of interpolation polynomial: 2, stator and rotor material non-linear, the maximum number of iterations Newton: 20, Newton tolerance of 1% and maximum tolerance is considerate potential values obtained by the conjugate gradient method, 0.01%. To refine the mesh refining technique to use adaptive setting a 15% share of refining.

As for the shaft material and its position in relation to the air gap, these variables were determined according to the induced electromotive. Changing the position of the shaft in relation is specific to machines that the air gap plain bearings and the bearings when they appear in the game.

2.2 Influence of unbalance magnetic circuit for the induced voltage

Because the main cause of tensions alternative from the shaft is from the unbalance magnetic circuit, they were shaped by interruption of rotor bars cage circuit. The number of interrupted bars changed and the position of the broken bars in the rotor circuit. Simulating a machine rotor winding at which a rotational phase is interrupted can also be performed using the numerical model of the motor in short, but the number of interrupted bars is 1/3 of the total number of bars, the position is properly selected according to the number of poles of the machine. Interruption of the two phases was also simulated by stopping the 2/3 of the rotor bars.

The following will present the results of numerical simulations for different values of the considered variables.

Figure 4 it shows the comparison, the change in electromotive tension induced in the machine shaft according to the number of bars broken, in case if the current in the stator windings is $0.2 \cdot I_n$ respectively $2 \cdot I_n$. It can be seen that the effect of unbalance (interrupted bars) is particularly important as the stator current is higher. A total of six broken rotor bars for a quarter machine, so 24 for the entire machine in the case of rotor in short, equivalent to a phase interruption for a winding rotor. Stator current values are considered small for startup mode, can only be achieved in practice when using a tool that allows controlling the current start.

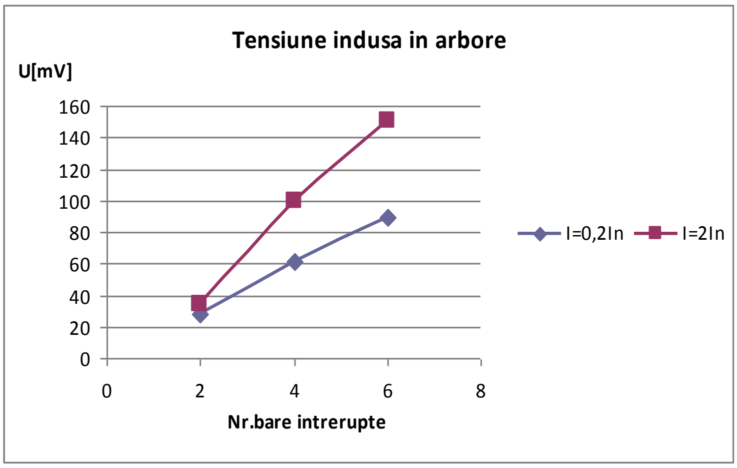

Fig. 4. The induced voltage according to the number of interrupted bars

Figure 5 represents the variation induced voltage based on the number of bars interrupted when the stator current has the value, $6I_n$, value that is common to start of asynchronous motors with the rotor in short-circuit.

The relative step of stator winding has no significant effect on induced voltage in the shaft, *Fig.6*. Voltage variation with relative step is insignificant.

The way in which the induced voltage changes according to magnetic permeability of the material it is made of the shaft shown in *Figure 7*. The case study corresponds to the initial current in value of $6I_n$, the position of the shaft is offset from the center of symmetry of the machine, with 1 mm on each of the two axes, two phases of the rotor is interrupted, *Figure 7a.*

In the above conditions, but with a single- rotor phase voltage variation interrupted relative magnetic permeability is shown in *Fig. 7b*.

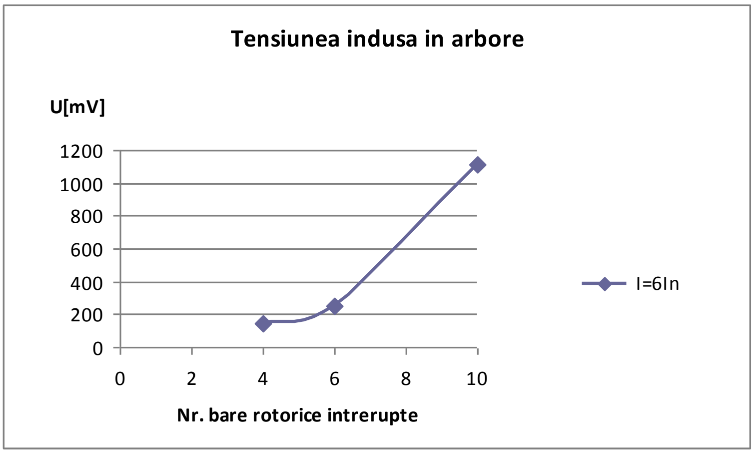

Fig. 5. Voltage induced on $6I_n$

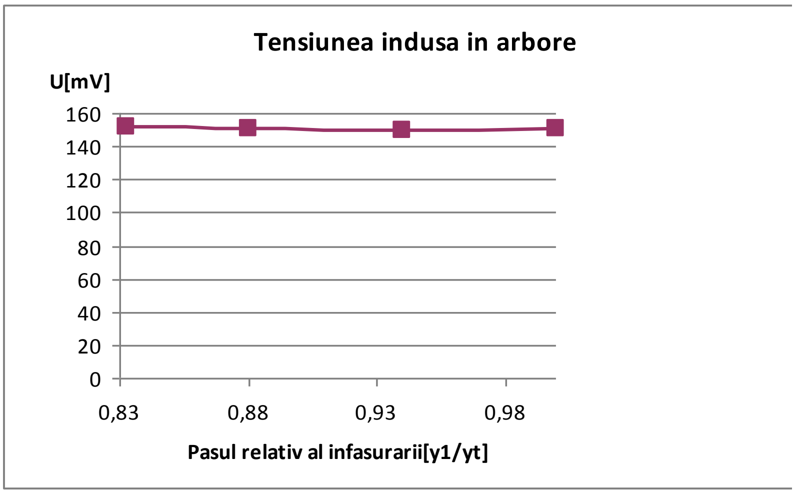

Fig. 6. Voltage depending on the relatively Step

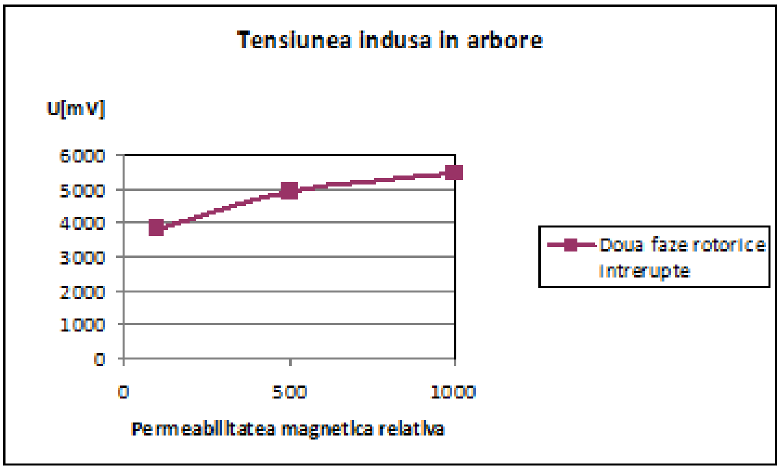

a) two interrupted phases

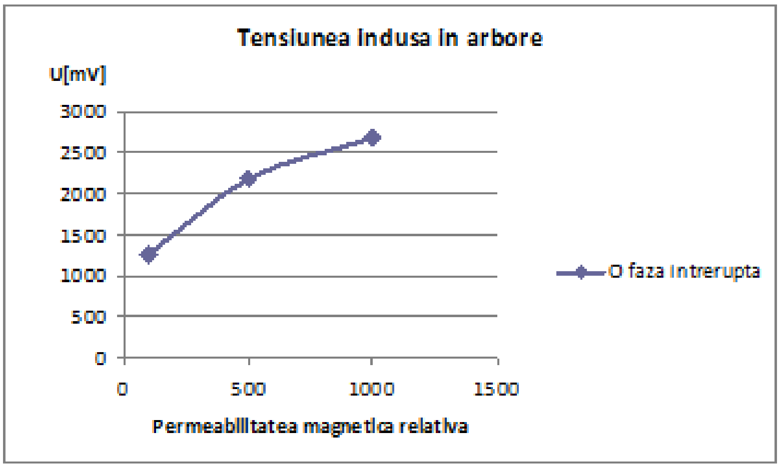

b) single interrupted phase

Fig. 7 The voltage depending on the permeability

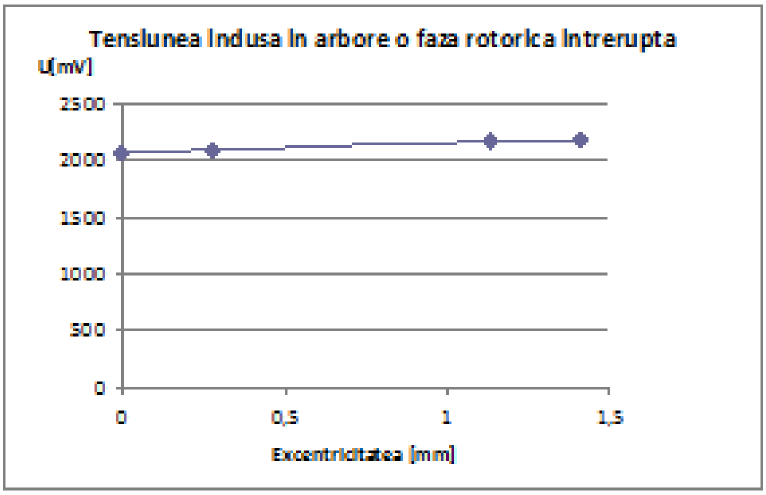

a) single interrupted phase

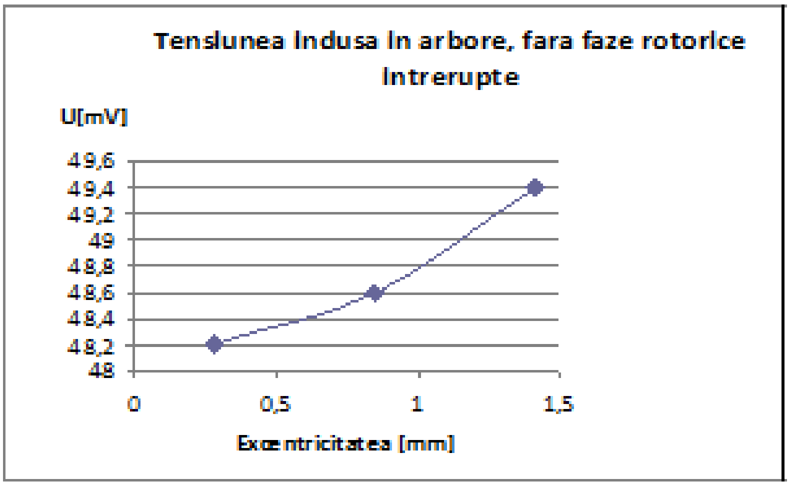

b) without interrupted phase

Fig. 8. The voltage depending on the eccentricity

Another parameter that can influence the value of the induced electromotive shaft is its displacement from the center of symmetry of the machine, i.e. eccentricity.

In *Fig. 8* was presented the dependency, if the current startup is $6I_n$, relative magnetic permeability of the material shaft is 500, and one rotor phase is suspended (a) and all phases are continuous (b).

As could be observed from the examples shown, the voltage induced in the shaft is influenced by the starting current. How it changes depending on the current stator in case we have 4 broken rotor bars and the machine shaft is offset from the center of symmetry with one millimeter on each axis is shown in *Fig. 9*

Form the induced voltage when starting the machine shaft, spindle being supported on bushings (eccentricity of 0.15 mm) obtained by simulations based on FEM is presented in *Figure 10*, and the resulting current through the camps equated with a capacitor is shown in

Fig.11. It can be observed the presence of harmonics of order 3 in the induced voltage. This was expected since the simulation was performed at a voltage of 220 V winding stator, the magnetic circuit of the machine being so saturated.

As will be seen in the case of measurements with increasing saturation, harmonic order 3 becomes increasingly important. The effect is that for voltages higher harmonics data bearing capacitive reactance decreases with increasing harmonic order, which will cause currents higher values than would be present for fundamental harmonic only.

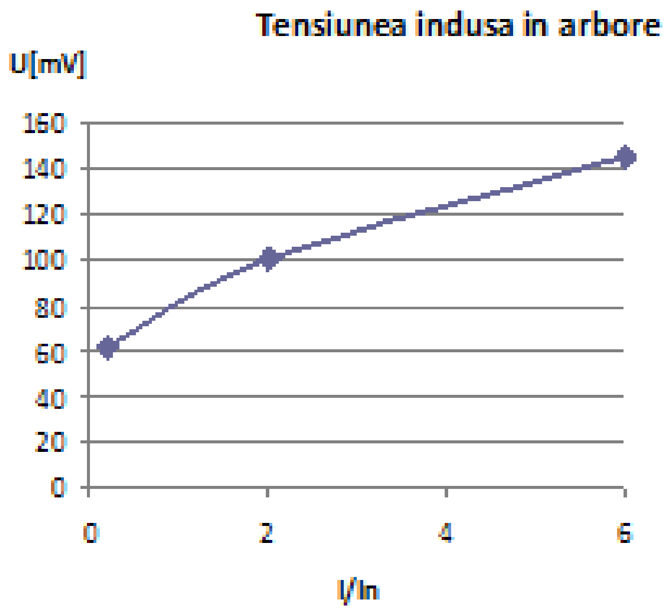

Fig. 9. The voltage induced by the starting current

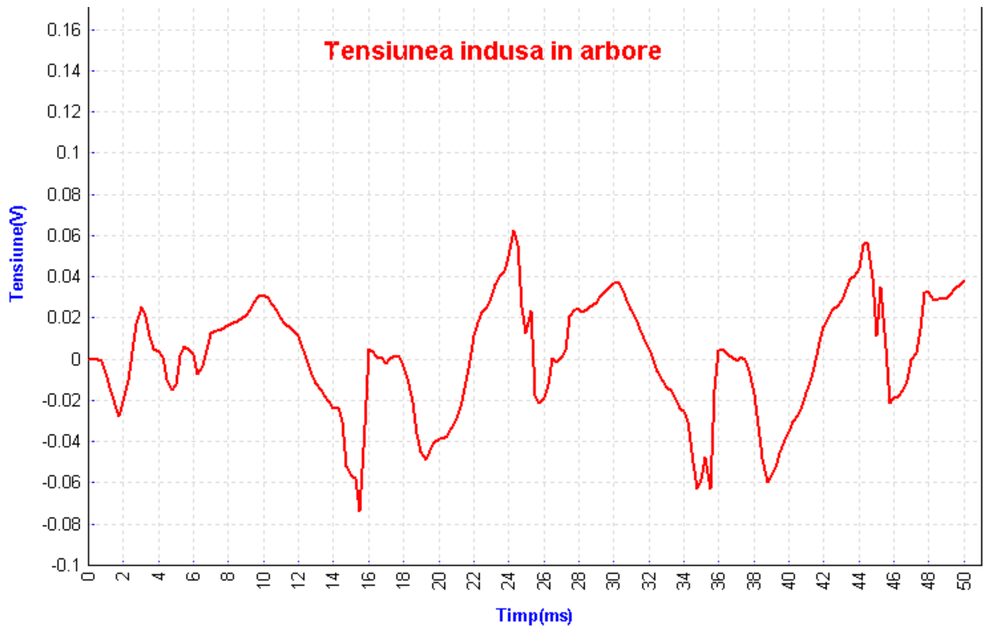

Fig. 10. The induced voltage form in the shaft

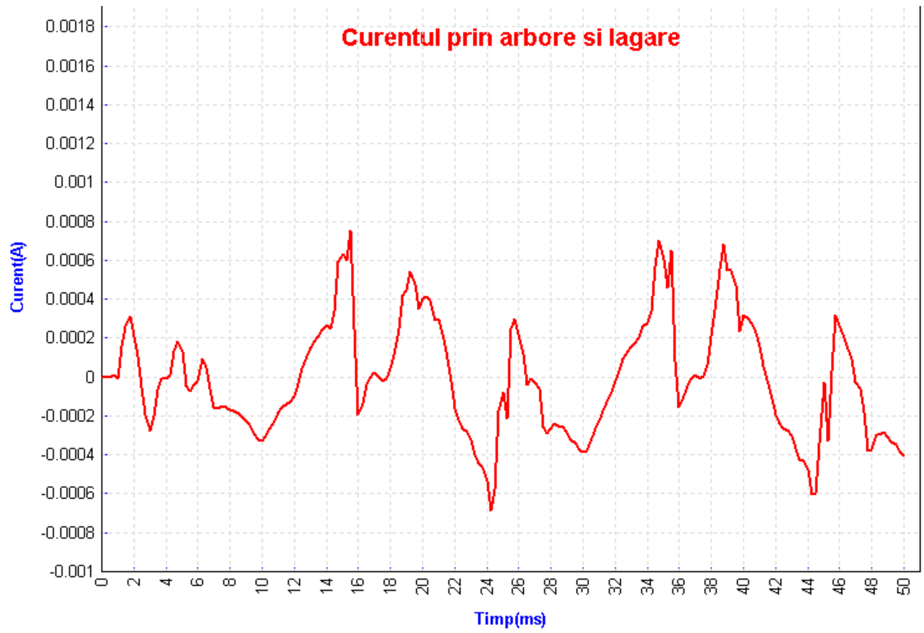

Fig. 11. Shape of current through the camp

3. CONCLUSIONS

From the presented above we can draw the following conclusions:

- machine shaft voltage induced depends insignificantly by the stator step up winding ;
- just moving along with the rotor shaft, from the center of symmetry of the machine, does not cause dangerous ternsions to the shaft. (they are in order of mV-olts) :

This is due to the reaction field current of the rotor, which shields the shaft, the coil field is no longer enter it, so it does not cause the occurrence of a significant electric voltage shaft;

- While starting current influences the induced voltage in the tree, only its value even with displacement from the center of symmetry, it can cause a significant tensions;
- only relative magnetic permeability of the shaft, in the absence of rotor winding defects, does not raise significant tensions therein.

As a general conclusion it can be stated that the main cause of tensions on significant. values in the electric machines shaft is unbalance of magnetic fields rotor. This unbalance may be caused either by different material properties of the magnetic portions of the rotor magnetic circuit, and in particular to some defect occurs in the circuit of rotor windings such as the discontinuation of the cage bars of one of the phases and the rotor winding . In such situations, it can be observed (*Fig. 5, 7 and 8*) that the dangerous tensions appear in the shaft, this time tensions are more influenced by other parameters considered in the present study.

Thus, for the case considered, where one phase of the armature winding stopped, the relative magnetic permeability of the rotor shaft 100, the induced voltage is 1.2 V, reaching a relative permeability of 1000, at value of 2, 65V.

Interruption of the two phases (or of a corresponding number of bars) may cause the relative permeability of the shaft based on the voltage up at 5.5V.

REFERENCES

1. Bianchi N., *Electrical machine analysis using finite elements*, CRC Press, 2005;

2. Chiver O., Horgoş M., Barz C., Pop E., *About end winding inductance computation of AC machines using FEM 3D*, Proc. of International Conference of the Carpathian Euro-regions specialists in industrial systems, North University of Baia Mare, May 21-23, 2008;

3. Chiver O., Barz C., Pop E., *Aspects regarding induction motors rotor parameters determination by FEA,* The 7th International Conference on Electromechanical and Power Systems, SIELMEN October 8-9, Iaşi, România, 2009,

4. Chiver O., Horgoş M., Barz C., Pop E., *Consideration about stator winding leakage inductances determination by FEA*, 5th International Conference on Electrical and Power Engineering, EPE08, Iaşi, România, Octombrie 2008;

5. **Drăgănescu O. Gh**., *Încercările maşinilor electrice rotative*, Ed. Tehnică, Bucureşti, 1987;

6. **Min-Fu Hsieh, You-Chiuan Hsu**, *Investigation on end winding inductance in motor stator windings,* IEEE Trans. on magnetics, vol 43, nr.6, June 2007

7**. Schram A., Gerling D**., *Analytical calculation of the end winding leakage inductance based on the solution of Neumann integrals*, IEEE International Symposium on Industrial electronics (ISIE) Conference, Dubrovnik, Kroatien, 20-23 June, 2005;

8. * * * MagNet 6.21, User's Guide;

9.;* * * FEMM User's Guide;

CONTRIBUTIONS TO THE STUDY OF THE DYNAMIC OPERATING REGIME OF AN ELECTROMAGNETIC VIBRATOR

Mircea **HORGOȘ**, Olivian **CHIVER,** Cristian **BARZ**
Technical University of Cluj-Napoca, North University Centre of Baia Mare
mircea.horgos@ubm.ro ; olivian.chiver@ubm.ro ; cristian.barz@ubm.ro

Key words: electromagnet; force; polynomial interpolation
Abstract*: This paper presents the results of the calculation of the maximum static force air gap dependence for a fixed magnetic circuit geometry, using the finite element method. This contributes to the writing of a dependency matrix of higher rank than that available in discrete simulation results, leading to the generation of analytic expressions of general nature and not subject to simplifying assumptions for the maximum static force of air gap variation*

1. INTRODUCTION

Although electromagnetic vibrators are much used in practice, they are not sufficiently studied from a theoretical perspective. While vibropercutant mechanical systems are much studied there are only a few studies in connection with electromagnetic systems and especially on the electromagnetic vibrator (VEM). To obtain results close to reality in the study of electromagnetic vibrators it is necessary to keep in mind that we are dealing with electromechanical systems and must start from the equations describing the behavior of the whole system.

2. CALCULATION OF THE FORCE OF ATTRACTION DEVELOPED BY AN ELECTROMAGNET

Knowing the flow, inductivity or permeation of an electromagnet one can determine the electromagnetic force of attraction developed by the formula:

$$F = -\frac{1}{2}\cdot\frac{\lambda}{sh^2(p\delta)}\cdot(N\cdot i)^2 = -\frac{1}{2}\cdot\frac{1}{\alpha\delta^2}\left(\frac{p\delta}{sh(p\delta)}\right)^2\cdot(N\cdot i)^2 \qquad (1)$$

and if we neglect dispersion ($\lambda \to 0$ and $p \to 0$), we obtain the force:

$$F = -\frac{1}{2\alpha}\left(\frac{Ni}{\delta}\right)^2. \qquad (2)$$

or

$$F = -\frac{1}{2}\cdot\frac{B^2\cdot 2S}{\mu_0} \qquad (3)$$

being found as the general expression of the force of attraction developed by an electromagnet.

3. RESULTS OF THE FEM ANALYSIS

The basic configuration of the electromagnet studied has as active materials the electrical steel sheet cold rolled CR 1010 column, yoke and armature and copper with electrical conductivity σ = 5.77 * 107 S / m for coils.

Analyses are performed, neglecting the hysteresis effect of magnetic materials, considering its behavior according to the magnetization curve and the winding current values ranging from 0.1 - 5 A.

Before the actual simulations the necessary degree of refining the mesh to avoid large time or system crashes was tested using the “step by step” method, but without significantly decreasing the analysis results, especially those concerning the calculation of forces. This led to the analysis of interpolation polynomials of the second order and a refinement of the mesh on the geometric configuration of the electromagnetic form shown in Figure 1. and 2. In fig. 1 is shown a mesh for column yoke and armature, and in Fig. Network of air gap 2 is played with a refining how best foot polar opposite.

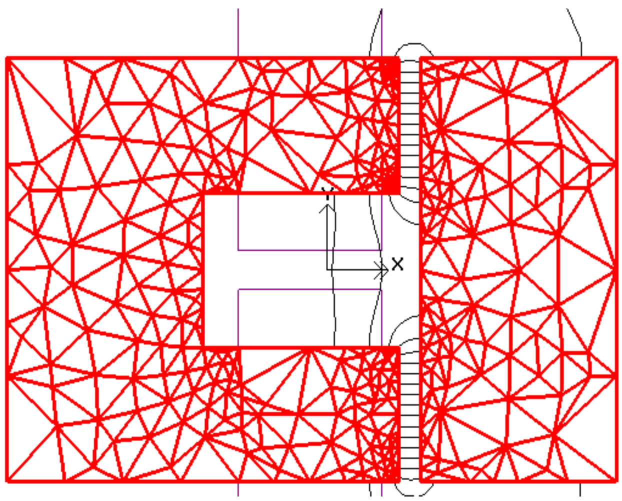

Fig. 1 Network and reinforcement mesh for column

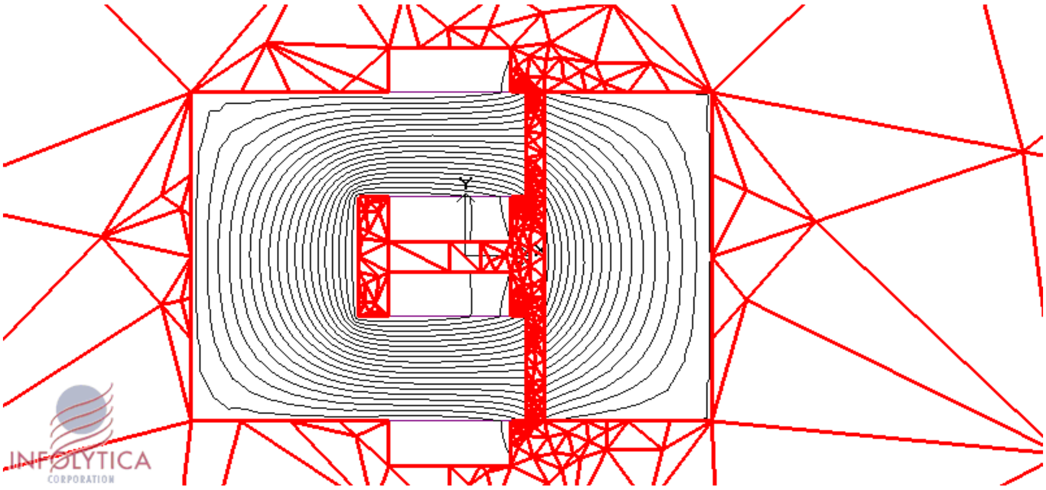

Fig. 2 The air gap mesh network

Below there are the results of the FEM analysis performed with the Infolytica MagNet software, version 6.11.

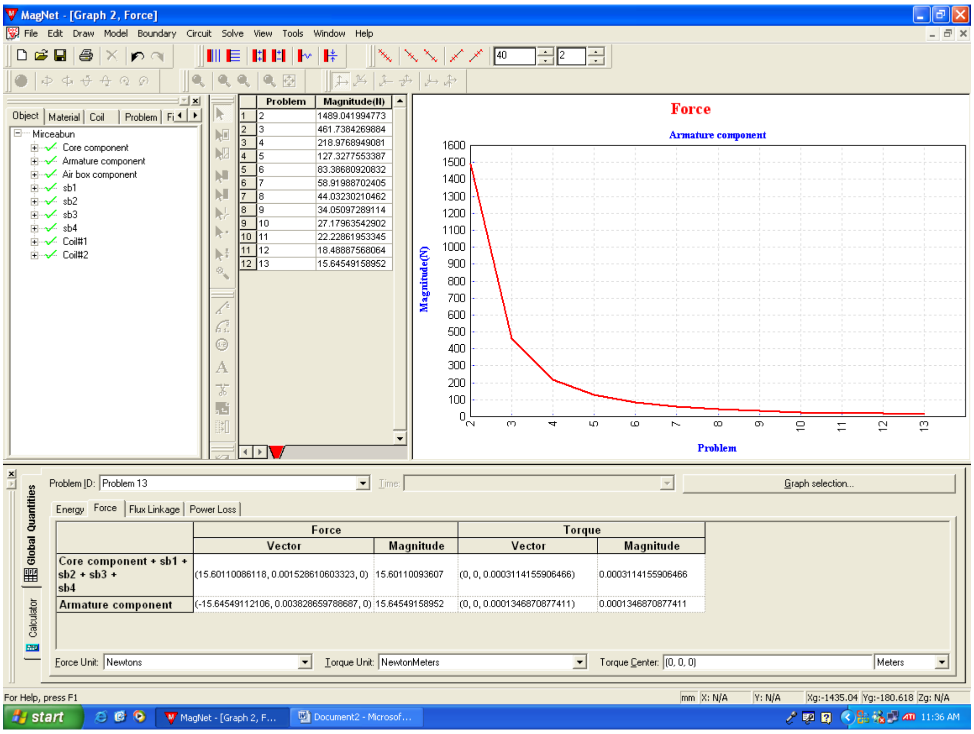

Fig. 3 Force characteristic for CR 10 and a current of 1 A

In the figure above the force chart is rendered, F = F (x) for varying air gap for the basic configuration of the electromagnet powered by a current of 1 A.

After analyzing all the models required and obtaining numerical results for each study model, we raised a family of characteristic curves of force for all configurations. Thus all air gap force characteristics could be analyzed comparatively according to size.

In the chart below force characteristics for current levels of between 0.1 - 0.5 A are given.

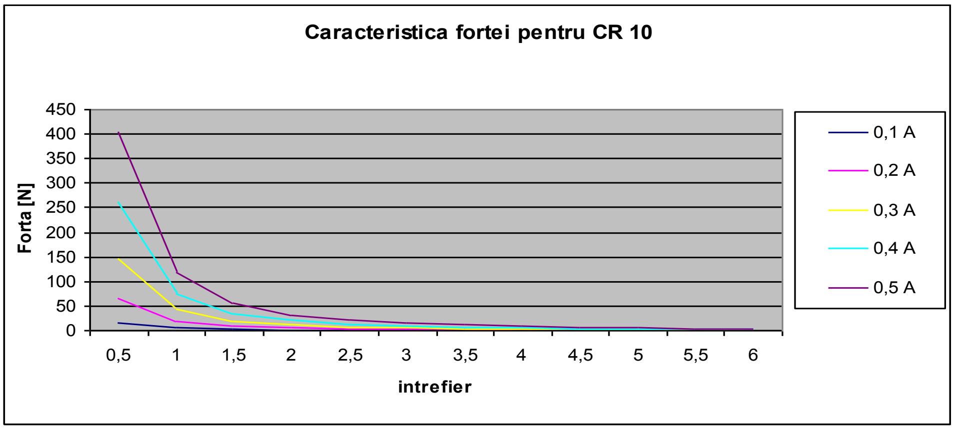

Fig. 4 Force characteristic for CR 10 and a current of 0.1 - 0.5 A

Accepting homogeneity and isotropy, at least in parts and assuming construction of finite elements so that they include inside an environment isotropic and homogeneous functional problems associated with such a perfectly valid both for linear and materials for nonlinear materials, noting that value is relative magnetic permeability is constant in the first case, be dependent on the value of magnetic induction, in the second.

The solution of a FEM analysis, of linear configurations is done simply by calculating the scalar magnetic potential values, similarly as the linear case, the values obtained representing the basis for the new values of the magnetic permeability of the magnetization curves. The cycle is repeated until the required convergence.

The study is conducted having as physical support of the electromagnetic phenomena nonlinear magnetic materials, linearity being considered only for the correlation of the presentation with intuitive aspects, analytically emphasizable, providing an overview of the phenomenology.

In general in usual design calculations, at least in the design phase of the basic model that optimization is later achieved on, linearity of magnetic materials is the key to solving them. This hypothesis is considered insignificant enough to attract errors, especially for small values of air gap, where the effect of magnetic saturation is smaller.

4. MAXIMUM FORCE STATIC DEPENDENCE AIR GAP

Based on the results of the FEM static simulation one can draw the maximum static force variation in the size of the air gap, with the parameter being the size the electric current i. Considering that the electromagnetic vibrator for which measurements were done, has the range of variation of current ranging from 0 to 3 A, we traced the curves F = F (x) for the following parameter values i = (0,3; 0,6; 1; 2; 3) A.

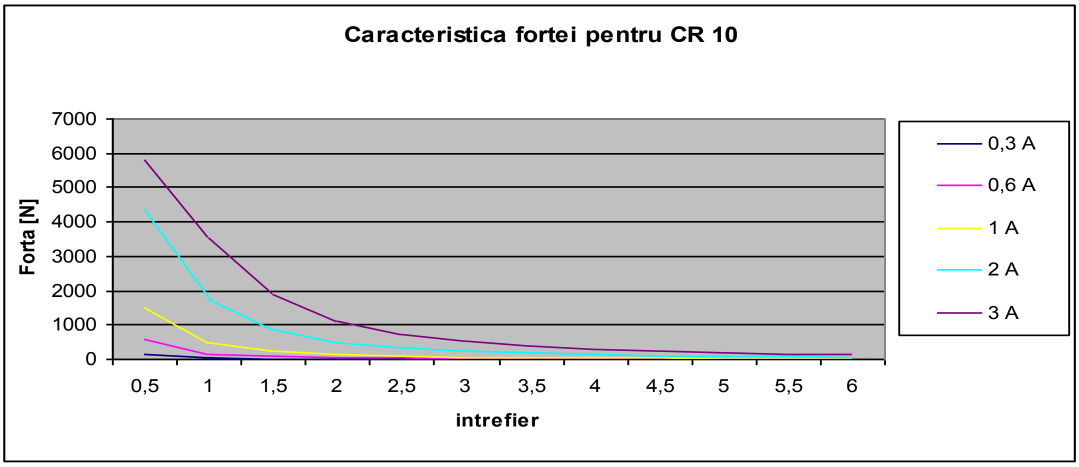

Fig. 5 Force characteristic for CR 10 and a current of 0.3 - 3 A

The shape is similar to a family of parabolas, for each value of *i* can easily determine the interpolation polynomial of the second order, which ensures a small deviation as:

$$F_{\max} = a_2 \cdot x^2 + a_1 \cdot x + a_0 \tag{4}$$

Identifying a polynomial interpolation requiring null values for the coefficients a_1 and a_0, transforms equation (4) in the expression of maximum static force air gap dependence for a fixed geometry and linear magnetic circuit, into the relationship:

$$F_{\max} = a_2 \cdot x^2 \tag{5}$$

By comparing the maximum static force on the one hand determined by FEM simulation and on the other hand by identifying the coefficient a_2 in equation (5) one can express some useful considerations early in the design calculations, especially regarding the influence of the assumption of magnetic materials linearity over the final outcome.

Based on the results of the FEM simulation, we can write the maximum static force air gap dependence for fixed magnetic circuit geometry in an analytic form. This form is useful; it helps one write a dependency matrix of higher rank than that available in discrete simulation results, leading to the generation of analytic expressions of a general nature and not subject to simplifying assumptions, for the maximum static force of air gap variation.

Obtaining the maximum static force value for any parameter value that expresses the geometry and electrical charge is essential for making a cover design method, and for the statistic deduction of dependency analytical formulas.

Thus, based on the existing data, also based on the polynomial interpolation, we determined, by using Matlab 6.5 tool, polynomial expressions which achieve, on the one hand the smallest residual norm, and on the other hand an overlap graph of the polynomial function over representation Fmax Fmax = (x) determined by FEM. For all the values of parameter *i*, second and fourth degree polynomials are obtained; these are shown in Fig. 6-8 respectively in Tables I - IV.

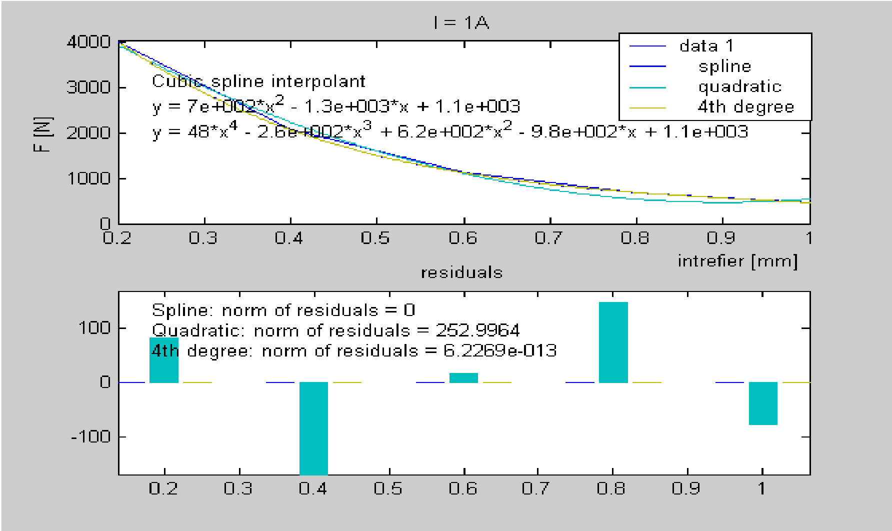

Fig. 6

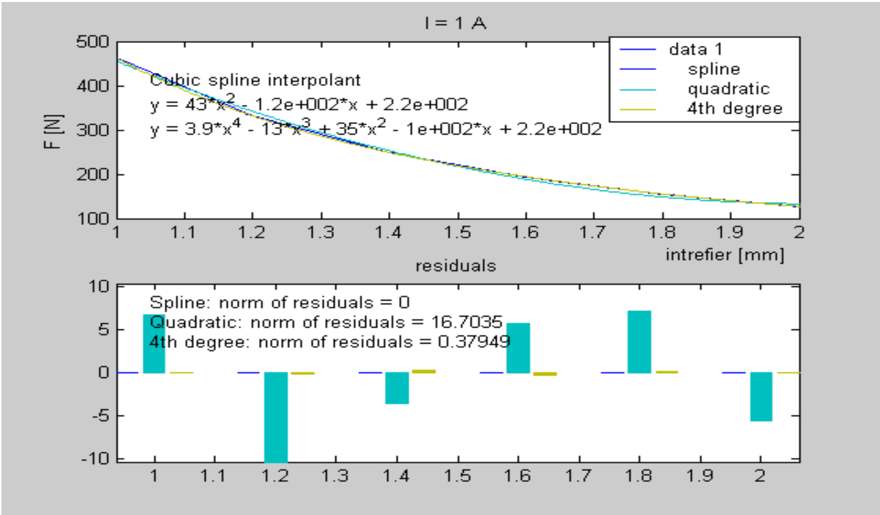

Fig. 7

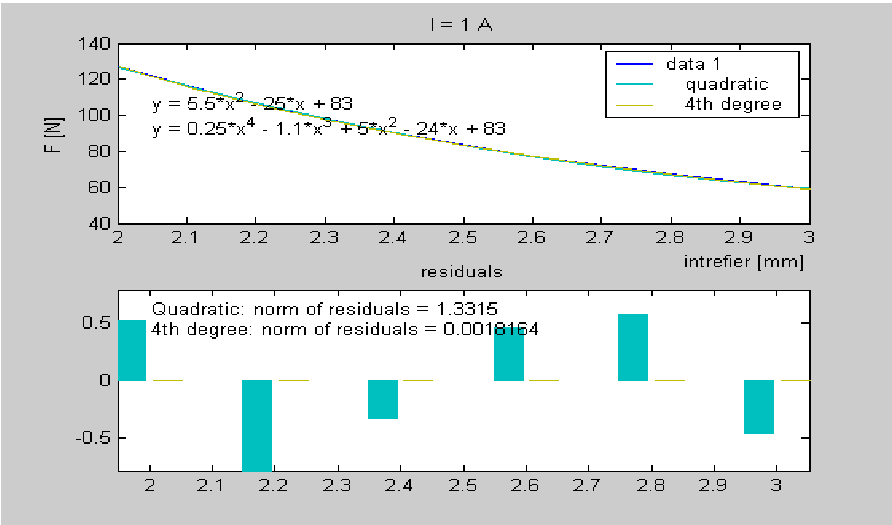

Fig. 8

Table I

i [A]	**Air gap 0 – 1 mm / Polynomials of degree two four**	**Norm of residuals**
0,3	1,5e+002*x^2-2,1e+002*x+90	91,316
	50*x^4-92*x^3+62*x^2-83*x+1,1e+002	7,32e-014
0,6	4,5e+002*x^2-6,9e+002*x+3,8e+002	243,736
	1,2e+002*x^4-2,5e+002*x^3+2,4e+002*x^2-3,5e+002*x+4,2e+002	5,28e-013
1	7e+002*x^2-1,3e+003*x+1,1e+003	252,997
	48*x^4-2,6e+002*x^3+6,2e+002*x^2-9,8e+002*x+1,1e+003	6,23e-013
2	1,4e+002*x^2-1,8e+003*x+3,7e+003	211,598
	47*x^4+2,2e+002*x^3+2,2e+002*x^2-2,1e+003*x+3,7e+003	2,53e-012
3	1,2e+002*x^2-1,3e+003*x+5,4e+003	23,569
	36*x^4+17*x^3-55*x^2-1,3e+003*x+5,3e+003	1,88e-012

Table 2

i [A]	**Air gap 1 – 2 mm / Polynomials of degree two four**	**Norm of residuals**
0,3	4*x^2-11*x+20	1,595
	0,38*x^4-1,3*x^3+3,3*x^2-9,2*x+20	3,9e-002
0,6	16*x^2-44*x+78	6,325
	1,5*x^4-5,1*x^3+13*x^2-37*x+79	0,152
1	43*x^2-1,2e+002*x+2,2e+002	16,704
	3,9*x^4-13*x^3+35*x^2-1e+002*x+2,2e+002	0,38
2	1,5e+002*x^2-4,5e+002*x+8,5e+002	54,685
	11*x^4-44*x^3+1,3e+002*x^2-3,9e+002*x+8,6e+002	1,044
3	2,5e+002*x^2-8,9e+002*x+1,9e+003	58,898
	0,38*x^4-48*x^3+2,6e+002*x^2-8,2e+002*x+1,9e+003	1,476

Table 3

i [A]	**Air gap 2 – 3 mm / Polynomials of degree two four**	**Norm of residuals**
0,3	0,5*x^2-2,3*x+7,5	0,12
	0,023*x^4-0,097*x^3+0,45*x^2-2,1*x+7,5	1,47e-004
0,6	2*x^2-9,1*x+30	0,482
	0,091*x^4-0,39*x^3+1,8*x^2-8,5*x+30	5,9e-004
1	5,5*x^2-25*x+83	1,332
	0,25*x^4-1,1*x^3+5*x^2-24*x+83	1,82e-003
2	21*x^2-99*x+3,3e+002	5,067
	0,94*x^4-4,1*x^3+19*x^2-94*x+3,3e+002	0,016
3	46*x^2-2,2e+002*x+7,4e+002	10,55
	1,9*x^4-8,5*x^3+42*x^2-2,1e+002*x+7,4e+002	0,014

Table 4

i **[A]**	**Air gap 1 – 3 mm / Polynomials of degree two four**	**Norm of residuals**
0,3	$5,4*x^2-11*x+11$	5,51
	$1*x^4-2,4*x^3+3*x^2-6,6*x+12$	0,523
0,6	$21*x^2-42*x+44$	21,918
	$4*x^4-9,6*x^3+12*x^2-27*x+46$	2,064
1	$58*x^2-1,2e+002*x+1,2e+002$	58,76
	$11*x^4-26*x^3+34*x^2-74*x+1,3e+002$	5,336
2	$2,1e+002*x^2-4,4e+002*x+4,9e-002$	204,02
	$35*x^4-90*x^3+1,3e+002*x^2-2,9e+002*x+5,1e+002$	15,895
3	$4e+002*x^2-9e+002*x+1,1e+003$	318,8
	$39*x^4-1,4e+002*x^3+3,1e+002*x^2-6,7e+002*x+1,1e+003$	6,423

From the analysis of the above figures and summarizing table, small deviations are observed for the entire range of variation of electric current.

In fact, despite the fact that the polynomial interpolation deviation from the results of the FEM analysis is small, the error of the linear behavior of the magnetic material can be considered unimportant up to a value of 1 mm air gap and an electrical load of 1 A. In this case, generating a geometric configuration VEM is acceptable, the model being easily optimized by FEM. Over a gap greater than 1 mm, the error resulting from the calculation of the maximum static force increases with the increase of the power application, as confirmed physically by the appearance of saturation.

The possibilities of "linearization of magnetic materials" subject to medium and large electrical applications, being relatively low due to saturation, the correction based on the model using coefficients having a relatively low degree of generality and less controllable precisions, the numerical analysis is required as a way of solving the nonlinear field problems.

The major disadvantage of numerical analyses dependent on many parameters is the occurrence of solutions as discrete representations, i.e. values to which the parameter values that led to these values must be linked. With the increasing number of parameters it is more difficult to express the solution in areas with continuous aspect (small ranges of variation of parameter values).

A particular case is the current study, which analyzes several models and where, in order to avoid obtaining a solution whose behavior in relation to the variation of the approached parameters is impossible to gauge, it was conducted in selected areas of their variation, i.e. chosen so as to cover optimal ranges of variation under the current technologies and materials.

5. CONCLUSIONS

Comparing the characteristics of the force obtained using the analytical calculation and data processing [4] and using the finite element method through the MagNet, we found out the following:

- both methods achieved a maximum strength for minimum air gap;
- the more the air gap increases, the more dramatically the force decreases;
- it was demonstrated by means of the two methods that the dynamic mode of operation of an electromagnet is the regime in which both the electric and magnetic quantities, and the mechanical ones vary simultaneously in time; it is the most general operation of an electromagnet, corresponding to a situation in which the moving fittings move, achieving the conversion of electric energy into mechanical energy;
- state quantities characterizing the dynamic regime of an electromagnet, while variable in time, independent or associated, are: the current, the flow, the force of attraction, the mobile fittings movement, (the air gap), speed and acceleration of the movement;
- the qualitative emphasis of these characteristic quantities is achieved most conveniently by computer graphics using methods based on the finite element theory.

REFERENCES

1. P. Andea, „*Electromagnetii*,” Editura Helicon, Timisoara, 1993

2. S. Darie, „*Vibratoare electrice*,” Editura Tehnica, Bucuresti, 1987

3. M. Ghinea, V. Fireteanu, „*Matlab, calcul numeric, grafica, aplicatii*,” Editura Teora, Bucuresti, 1995

4. M. Horgos, L. Neamt, O. Chiver, Z. Erdei, „*Contributions to the calculation of the forces developed by the electromagnets using FEM*,” International Multidisciplinary Conference 7th Edition, Baia Mare, Romania, Scientific Bulletin Seria C, Vol. XIX, Fascicle: Mechanics, Tribology, Machine Manufacturing Technology, May 17-18, 2007, pp. 273 – 278

5. L. Neamt, A. Neamt, M. Horgos, „*The influence of the magnetic non-linearity on the magnetostatic shields design*”, Rev. Roum. Sci. Techn. - Electrotechn. Et Energ., 53, Bucharest, 2008

6. [***] *An introduction for Infolyitica Magnet 6.11*

PROGRAM FOR THREE-PHASE POWER TRANSFORMER DESIGN

Olivian **CHIVER**, Eleonora **POP** and Ionut **BARSAN**
North University of Baia Mare, Department of Electrical, Electronics and Computers Engineering, olivian.chiver@ubm.ro

Key words: finite, elements, power, transformers, design
Abstract*: This paper presents a program developed for designing three-phase power transformers used in power systems. The program was developed in Visual Basic because this programming language allows us to realize a friendly and suggestive interface with minimum effort. The second reason, which is the most important, is to use Visual Basic, because this language is recognized by the used finite elements analysis (FEA) software, MagNet produced by Infolytica. This software package is designed for calculation of the magnetic field of electromagnetic devices and machines. The 3D components of the numerical model are carried out using CATIA program, automatically, based on the calculated main geometric data.*

1. INTRODUCTION

As it is known the design requires laborious calculations for sizing and verification, calculations for determining the parameters, comparing them with those required by the theme, the return to an earlier stage and choosing other values of the possible, restoration and re-checking calculations, and optimization chosen option.

Once completed, this first step of the design must be checked by simulations of the chosen option. These simulations must confirm the analytical calculations and allow the determination with accuracy of the parameters of the designed device.

Currently, one of the most used methods for simulating electromagnetic machines and devices is the finite elements method. It is widely accepted, verified and confirmed that finite elements method allows obtaining accurate results if the user of the program is well informed of both the operating mode of the program, the principles underlying the method, and the phenomena that occur in the designed device.

Given all this, it is obvious that in order to get a quality apparatus it is necessary that several possible options need to be designed, optimized, analyzed and compared. Computer aided design is the one that solves this problem because it allows, in a short time and with minimal effort, to get more options that meet the requirements imposed by the design theme.

In case of the power transformers, the design calculus is relatively well set, but, depending on how the designer choose certain parameters/dimensions at some point, and depending on the used materials, it can get more options that meet the conditions imposed by the theme. The final decision should always be the one that takes into account both the technical and the economic aspects to finally obtain the best quality/price.

2. THE PROGRAM DESCRIPTION

The developed program is an application that is based on the programming language Visual Basic, and runs under the used numerical analysis program, MagNet. Based on the data calculated in the design phase, a 3D numerical model of the transformer is automatically performed. The analysis of the performed model, enables the transformer parameters determination, the transformer characteristics determination, and the study of some transients regimes such as no-load network connection and sudden short circuit regime.

Main design data of a three-phase power transformer are the rated voltages of primary and secondary phases, the winding connections, the phase-angle displacement between primary and secondary terminals, winding material, nominal apparent power, etc. Other parameters imposed by theme are nominal losses and the short circuit voltage.

Figure 1 shows the program interface. The design data are taken from text boxes when the button "Proiectare" is clicked, and the interaction with the user of the program (designer) is done through the dialog boxes. In the dialog boxes are messages about the parameters which must be established, and information obtained by calculation regarding the recommended value or range of values, out of which the finale value must be chosen, fig. 2.

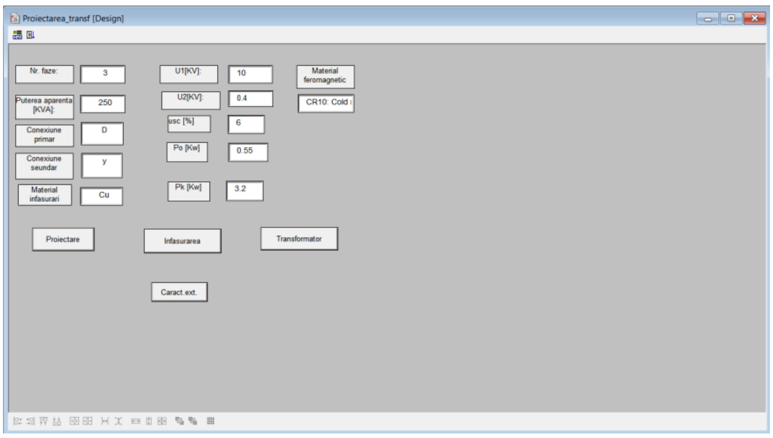

Fig. 1–Program interface

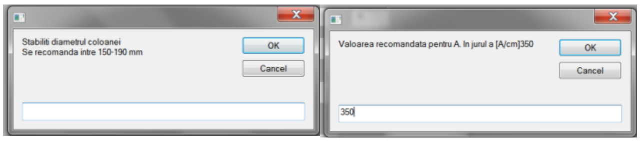

Fig.2 Dialog box

The values set out in dialog box are finale values for that parameter.

Message boxes are also used to inform the designer on the calculated value of a parameter at a time.

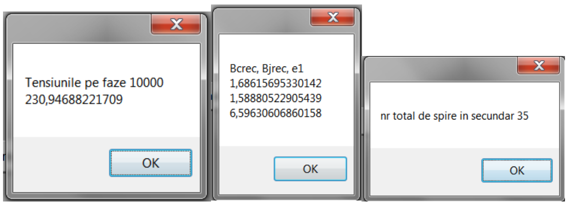

Fig.3. Message box

In case that the quantities do not meet certain conditions imposed by the theme, the message box displays this, and the program returns to the point where we must make changes, fig. 4.

Fig. 4 Conditions are not satisfied. Tips are suggested

The main geometric dimensions once determined, clicking the button "Infasurare" it is created one column of the transformer and the corresponding two windings, Fig. 5.At this moment, the column is performed with circular section, but in the future we want that the program realizes columns/yokes with steps shaped section.

Also, the lamellar construction of the magnetic circuit is defined by the material properties, not by the manner of the transformer magnetic circuit realization in 3D numerical model.

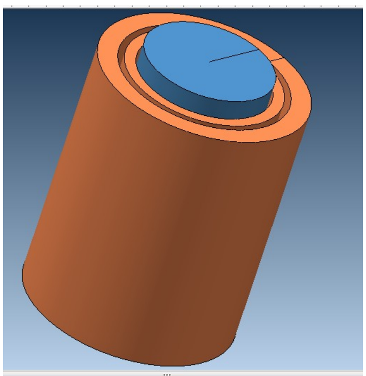

Fig. 5 Column and corresponding windings

Then, clicking the "Transformator" button, the whole transformer (with corresponding columns, yokes and windings) is constructed, fig. 6. At this time the program does not automatically set the number of turns of the windings, this should be done by the user, fig. 7.In the future we will add features to do this automatically, based on the design calculated data.

Also, the boundaries of the calculus domain and the boundary conditions should be set by the user. In this case an air box around the transformer has been built, fig. 8, so that the leakage flux is not diminished, and the established boundary conditions were "tangential flux".

The initial mesh is showed in fig.9.

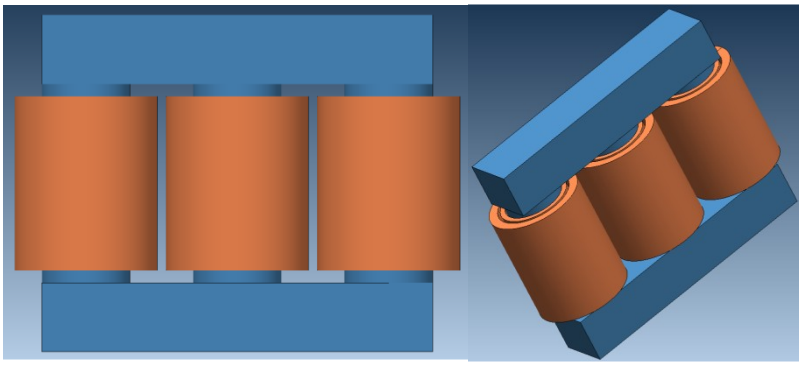

Fig.6 The whole transformer

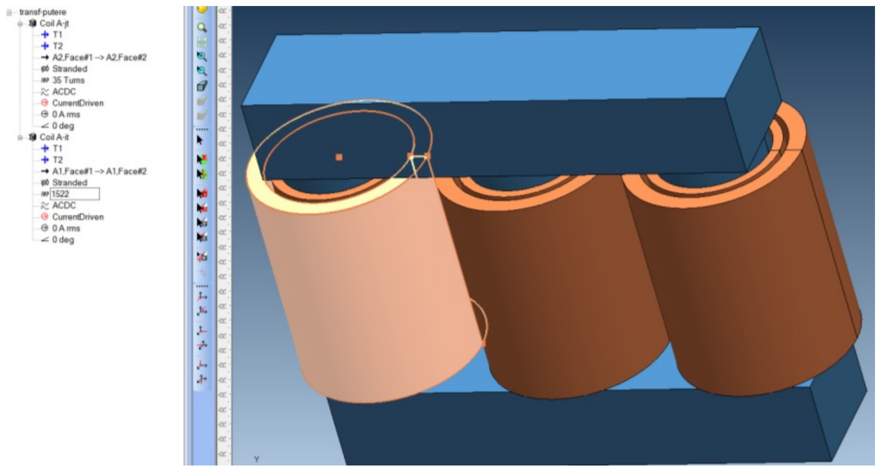

Fig. 7 Turns number of the windings establishment

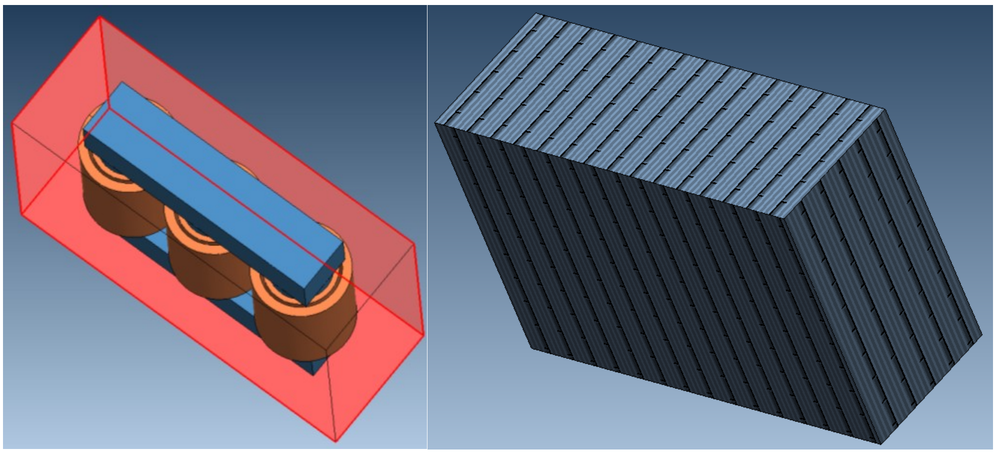

Fig. 8 Airbox and boundary condition

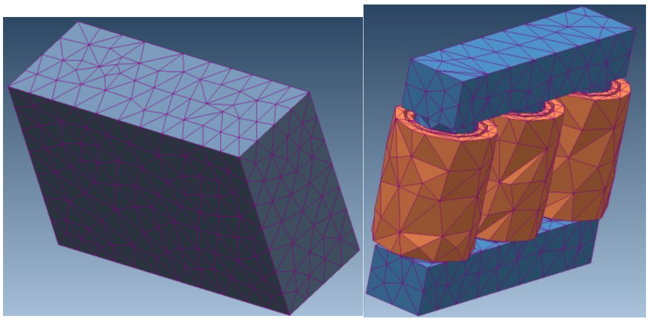

Fig. 9 Initial mesh; air box and transformer

3. MAGNETIZING AND LEAKAGE INDUCTANCES DETERMINATION

Leakage inductances of the transformer can be determined by finite elements analysis as described in the following. The imposed winding currents must satisfy the relation,

$$N_1 I_1 = -N_2 I_2, \tag{1}$$

where N_1 and $N_2$are the turns number per phase for primary winding and secondary winding respectively, and I_1 and $I_2$are the rms phase current of primary winding and secondary winding respectively. The primary and secondary phase (A-a, B-b and C-c) currents must be in relation,

$$I_{A,a} + I_{B,b} + I_{C,c} = 0, \tag{2}$$

A 3D magnetostatic analysis may be performed and the currents are in relation,

$$\frac{I_{A,a}}{2} = -I_{B,b} = -I_{C,c}, \tag{3}$$

Because the magnetic circuit is non-saturated, the phase leakage inductance (the short-circuit phase inductance) can be determined from the magnetic energy stored in the whole domain with relation,

$$L_{sc} = L_{\sigma A} + L_{\sigma a}^{'} = \frac{4}{3}\frac{W}{I_A^2}, \tag{4}$$

In this case, the separation of the primary leakage inductance from the secondary leakage can be performed considering them equal or in the same ratio with the resistances.

Also, since at short circuit regime each phase winding is linked only with its own magnetic flux, leakage inductance of each winding can be determined as the ratio between the magnetic flux and the winding current. In this case, all computed inductances are not in reported values.

The magnetizing inductance depends on the value of the supplied voltage. Determination of the magnetizing inductance can be achieved for any value of the supply voltage, proceeding as follows. The primary phase winding will be feed by voltage sources, being careful that winding resistance to be equal to that analytically calculated (or real one). If the harmonic analysis at rated frequency is performed, the phase currents will result(secondary being no load).The ratio between voltage and current of one phase represents the phase impedance. Since the phase resistance is known, one can determine the phase reactance and inductance respectively. The inductance determined in this way is the sum of the magnetizing inductance and leakage inductance of one phase.

The numerical model once performed, all the transformer characteristics can be determined by simulations, the transient regimes can be studied and also the influence of the winding connections on the no-load regime or unbalanced regime scan be studied.

4. CONCLUSIONS

The design program of three-phase power transformer is a useful tool in computer aided design of these devices. Based on the classic design, after establishing geometric configurations, the numerical model required to 3D finite element analysis can be achieved. Finite elements analysis program allows the simulation of all stationary or transient operating regimes encountered in the operation of power transformers, the accuracy of the results being dependent on the accuracy of the performed numerical model and the analysis conditions set by user. Finally, it must be specified that the interpretation of the numerically obtained results and then their usage for the determination of some parameters, or the transformer parameters variation in certain conditions, requires that the user knows very well the characteristic phenomena of the analysed device.

REFERENCES

1. **N. Bianchi**, *Electrical machine analysis using finite elements*, CRC Press, Taylor & Francis Group, 6000 Broken Sound Parkway NW, Suite 300, 2005.

2. I. Cioc, C. Nica, *Proiectarea maşinilor electrice*, Ed. Tehnică, Bucuresti 1994.

3. O. Chiver, L. Neamt, M. Horgos, *Finite Elements Analysis of a Shell-Type Transformer,* Journal of electrical and electronics engineering, Vol4/nr.2/2011.

4. K.Karsai, D.Kerenyi and L.Kiss, *Large power transformers*, Hungary, Elsevier, 1987.

5. A. Naderian-Jahromi, Jawad Faiz and Hossein Mohseni, *Calculation of distribution transformer leakage reactance using energy technique*, Australasian Universities Power Engineering Conference, AUPEC 2002.

6.***MagNet user's guide.*

7. www.infolytica.com.

FUZZY LOGIC CONTROL

Zoltan **ERDEI**, Paul **BORLAN**
North University of Baia Mare, Eaton Electroproduction Romania
zoltan.erdei@cunbm.utcluj.ro, borlan.paul@gmail.com.

Key words:control, fuzzy logic, fuzzy logic control

Abstract*: In this paper the authors present the usefulness of fuzzy logic in controlling engineering processes or applications. Although fuzzy logic does not represent a novelty for the scientific and engineering field, it enjoys a great appreciation from those involved in the two domains. The fact that fuzzy logic uses sentences kindred with the natural language make it easier to comprehend that a complex mathematical model required by the classic control theory. In MatLab software there are dedicated toolboxes to this subject that make the design of a fuzzy controller a facile one. In the paper design methods of a fuzzy controller are being presented both in Simulink and MatLab.*

1. INTRODUCTION

Every day we can observe how our daily activity becomes more dependent of computers and electronic devices in order to control resources and processes from the real world.

Such an example can be seen on airports all around the world, where a plane pilot receives indications in order to land or take off safely, without the flight controller having to look on the window.

Soft computational approaches in decision making have grown in popularity in many fields. This is easily observed by the large number of technical papers that are published in journals and magazines as a result of conferences in all domains of engineering, production, science, medicine and business. Soft computational method is a fast evolving field and it implies knowledge, technics and methods from various sources.

We have chosen this subject for our paper because soft computational methods have a large applicability in the field of engineering and control, and also due to the fact that they are highly appreciated by engineers. Also there is dedicated software that gives a special attention to these technics, such as tools and toolboxes. For example in MatLab for fuzzy logic we have Fuzzy Logic Toolbox and for neural networks we have Neural Network Toolbox.

2. FUZZY CONTROL

Fuzzy logic controllers satisfy the same functions as conventional controllers, but they handle more complex control problems by heuristic models and mathematics given by the fuzzy logic, rather than mathematical models given by differential equations.

An approach for fuzzy control is a functional form of the fuzzy system, developed by Takagi and Sugeno, where there is no need for defuzzification. This model based fuzzy control method can be used when it is possible to describe the system's dynamics at a local level in adequate terms.

The main rule of the method is

$$R_j : If\ x_1\ is\ A_{j1}\ and\ \ldots\ and\ x_n\ is\ A_{jn}\ then\ u_j = f_j(x_1, x_2, \ldots, x_n) \tag{1}$$

for $j = 1,2,\ldots,r$, where x_i represents the observed values of the input variables, f_j are functions and A_{ij} forms a fuzzy partition of the input system. Considering the product of A_{ij} we can express the rules in a more simple form

$$R_j : „If\ \boldsymbol{x}\ is\ A_j\ then\ u_j = f_j(x_1, x_2, \ldots, x_n)” \tag{2}$$

The total output value is

$$u(x) = \sum_{j=1}^{r} A_j(x) f_j(x) \Big/ \sum_{j=1}^{r} A_j(x) \tag{3}$$

In the case of Takagi – Sugeno method each function f_j is liniar.

$$f_j(x_1, x_2, \ldots, x_n) = a_{0j} + \sum_{i=1}^{n} \alpha_{ij} x_i \tag{4}$$

Other used forms are the quadratic

$$f_j(x_1, x_2, \ldots, x_n) = a_{0j} + \sum_{i=1}^{n} a_{ij} x_i^2 \tag{5}$$

And the trigonometric

$$f_j(x_1, x_2, \ldots, x_n) = \exp\left(\sum_{ij}^{n} \alpha_{ij} \sin x_i\right) \tag{6}$$

When choosing $f_j(\boldsymbol{x})$ we must take into consideration the particularities of the application.

3. TAKAGI – SUGENO FUZZY CONTROLLER

In this example we will design a fuzzy controller that respects the requirements of the Takagi – Sugeno controller. The design has been made in MatLab Simulink.

This controller has 2 inputs and an exit. First input is given by the error, *error=x*, and the second is given by the time differential of the error, *error_dot=y*. The output of the controller is the change in the control action and not the control itself.

The fuzzy membership functions for the primary and secondary inputs are isosceles triangular, 5 membership functions for each input. The membership function for the first entry has its peaks at $[-\mathrm{x_a}\ -x_a/2\ \ 0\ \ x_a/2\ x_a]$. The base of each triangle has a length of x_a. The triangular function for the second entry has its peaks at $[-y_a\ -y_a/2\ \ 0\ \ y_a/2\ y_a]$. The base of each triangle has a length of y_a. x_a and y_a have been set at 1. The output membership functions are NB (negative big), NM (negative medium), Z (zero), PM (positive medium) and PB (positive big).

The fuzzy rules are:

$$\begin{aligned}
&R_{ij}, i = 1, \ldots, 5; j = 1, \ldots, 5 \\
&R_{11}: Dacă\ x\ este\ NB\ și\ y\ este\ NB\ atunci\ z\ este\ NB \\
&R_{12}: Dacă\ x\ este\ NB\ și\ y\ este\ NM\ atunci\ z\ este\ NB \\
&\vdots
\end{aligned} \tag{7}$$

Output *z* is calculated according to

$$z = \sum w_{ij} z_{ij} / \sum w_{ij}\ , i = 1, \ldots, 5; j = 1, \ldots, 5 \tag{8}$$

w_{ij} represents the weigh of the rule ij (minimum between the membership degree of input 1 and the membership degree of input 2). z_{ij} is the value of *z* in rule ij.

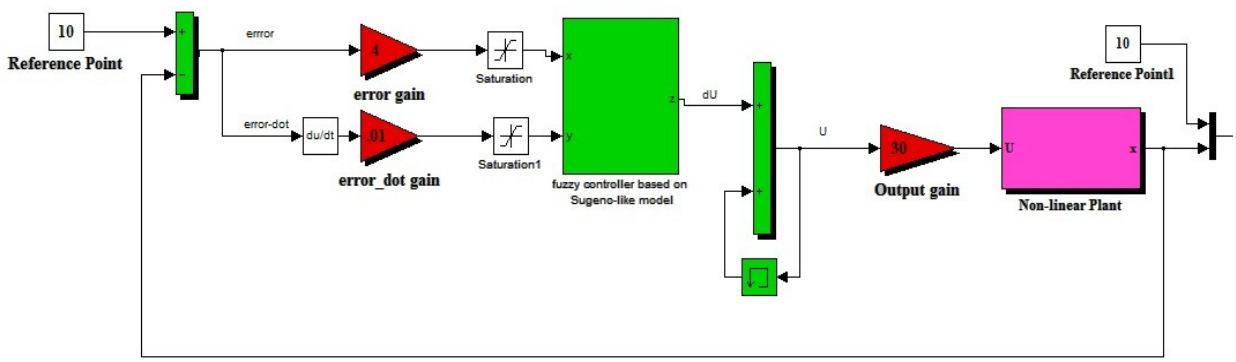

Fig 1. Block diagram of the Takagi – Sugeno controller

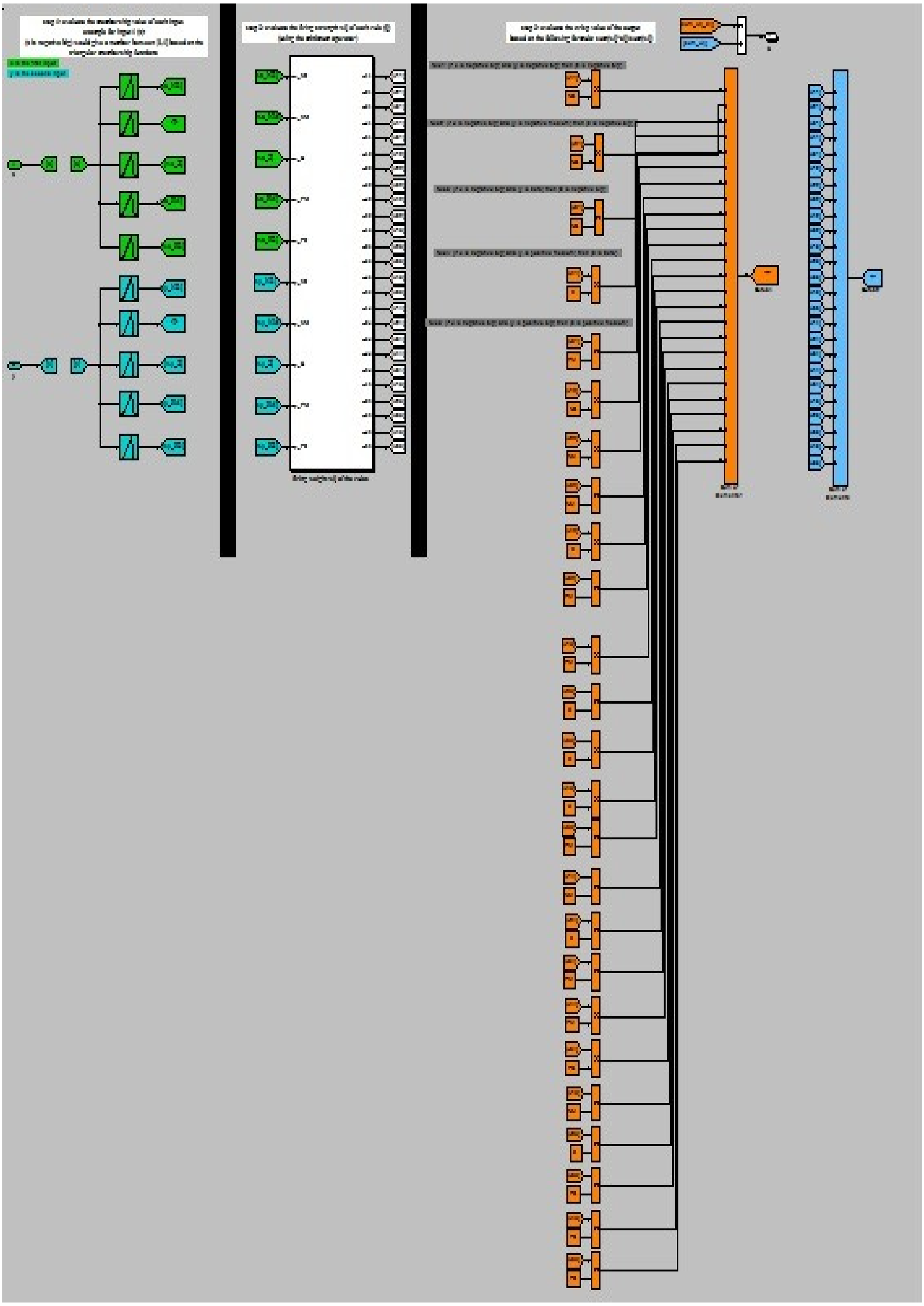

Fig. 2. The model of the controller

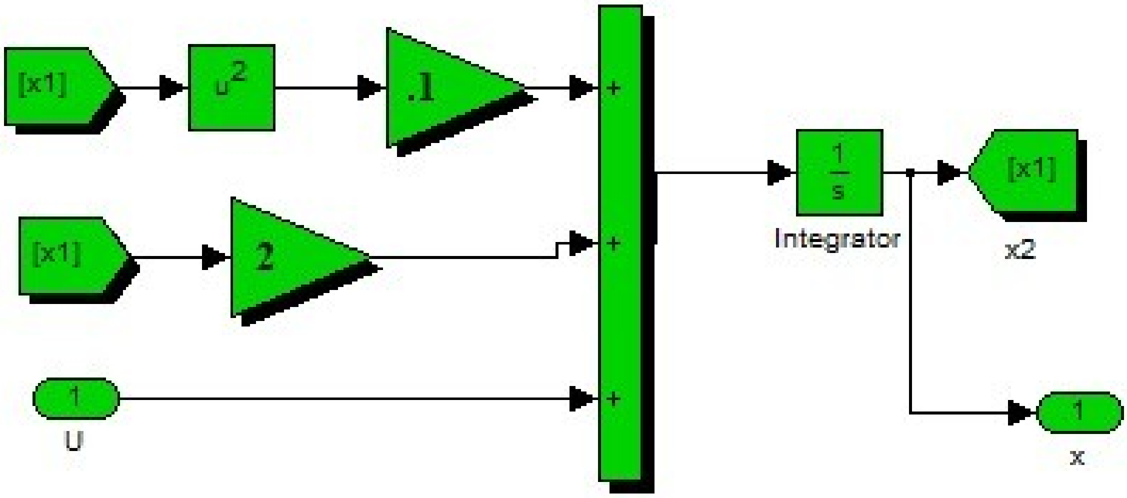

Fig. 3. The model of the system

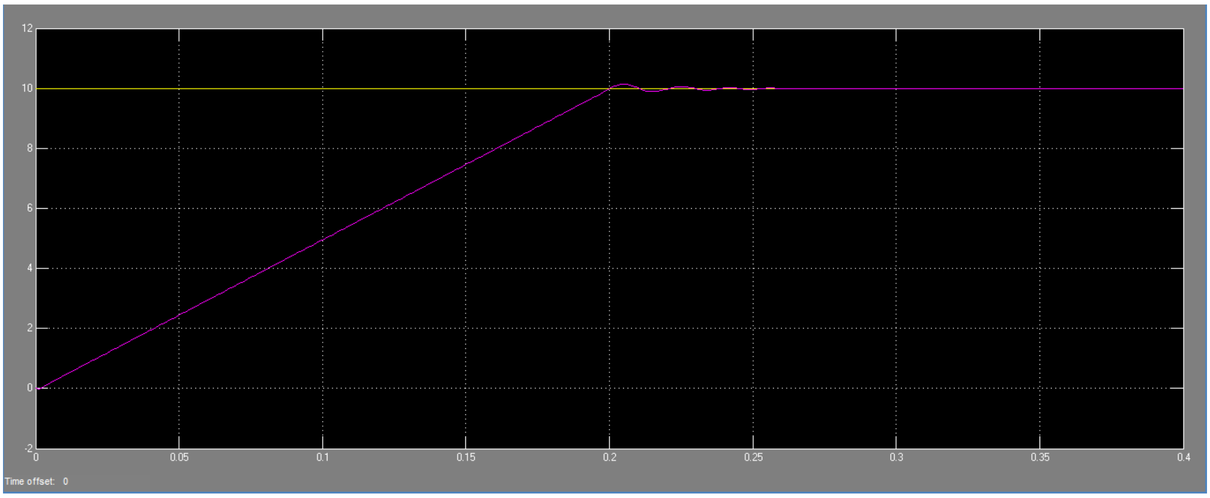

Fig. 4. The output of the controller

4. CONCLUSIONS

As it can be observed in the upper graph rises linearly to the desired value, and once this value is achieved there are fluctuations from the target, and through fuzzy control this value is manipulated and in this way we can obtain what we want from the system.

REFERENCES

1. **S. Abe and M.S. Lan**, *A method for fuzzy rule extraction directly from numerical data and its application to pattern recognition*, IEEE Trans. On Fuzzy Systems, 3, 18-28, 1995.
2. **G. Bojadziev and M. Bojadziev**, *Fuzzy Sets, Fuzzy Logic*, Applications, World ScientiÞc, London, 1995.

3. **E. Czogała and J. Łeþski**, *Fuzzy and Neuro-Fuzzy Intelligent Systems*, Springer-Verlag, Berlin, 2000.
4. **C.W. de Silva**, *Intelligent Control: Fuzzy Logic Applications*, CRC Press, Boca Raton, FL, 1995.
5. **R.C. Dorf**, ed., *The Electrical Engineering Handbook*, CRC Press, Boca Raton, FL, 1993.
6. **K. Dutton, S. Thompson, and B. Barraclough**, *The Art of Control Engineering*, Addison-Wesley Longman, Ltd., Essex, UK, 1997.
7. **M. Gehrke, C.L. Walker, and E.A. Walker**, *Normal forms and truth tables for fuzzy logics*, chapter in Proceedings of Linz 2000 Conference, Fuzzy Sets and Systems,2000.
8. **G.C. Goodwin, S.F. Graebe, and M.E. Salgado**, *Control System Design*, Prentice-Hall, Upper Saddle River, NJ, 2001.
9. **F. Höppner, F. Klawonn, and R. Kruse**, *Fuzzy Cluster Analysis*, JohnWiley & Sons, New York, 1999.
10. **J.S.R. Jang**, *ANFIS: adaptive-network-based fuzzy inference system*, IEEE Transactions on Systems, Man and Cybernetics, 23(3), 665-684, 1993.
11. **S.V. Kartalpoulos**, *Understanding Neural Networks and Fuzzy Logic*, IEEE Press, Piscataway, NJ, 1996.
12. **R.J. Marks** II, ed., *Fuzzy Logic Technology, and Applications*, IEEE Technology Update Series, IEEE Press, Piscataway, NJ, 1994.
13. **H.T. Nguyen, M. Sugeno, and R. Yager**, eds., *Theoretical Aspects of Fuzzy Control*, John Wiley & Sons, New York, 1995.
14. **H.T. Nguyen and E.A.Walker**, *A First Course in Fuzzy Logic,* 2nd Edition, CRC Press, Boca Raton, FL, 1999.
15. **K.M. Passino and S. Yurkovich**, *Fuzzy Control*, Addison-Wesley Longman, Menlo Park, CA, 1998.
16. **W. Pedrycz**, *Fuzzy Sets Engineering*, CRC Press, Boca Raton, FL, 1995.
17. **C.L. Phillips and R.D. Harbor**, *Feedback Control Systems*, 4th Edition, Prentice-Hall, Upper Saddle River, NJ, 2000.
18. **T.J. Ross**, *Fuzzy Logic with Engineering Applications*, McGraw-Hill, New York, 1995.
19. **M. Sugeno**, *Fuzzy Measure and Fuzzy Integral*, Trans. SICE, 8(2), 95-102, 1972.
20. **T. Takagi and M. Sugeno**, *Fuzzy identifcation of systems and its applications to modeling and control*, IEEE Trans. Systems, Man and Cybernetics, 15(1), 116-132, 1985.
21. **K. Tanaka and M. Sugeno**, *Stability analysis and design of fuzzy control systems*, Fuzzy Sets and Systems, 45, 135-150, 1992.
22. **K. Uehara and M. Fujise**, *Fuzzy inference based on families of alpha-level sets*, IEEE-Transactions on Fuzzy Systems, 1(2), 111-24, May 1993.
23. **L.X. Wang**, *Fuzzy systems are universal approximators*, Proceedings of the First IEEE Conference on Fuzzy Systems, San Diego, CA, 1163-1170, March 1992.
24. **B. Werners**, *An interactive fuzzy programming system*, *Fuzzy Sets and Systems*, 23, 131-147, 1987.
25. **R.R. Yager**, *On a general class of fuzzy connectives, Fuzzy Sets and Systems*, 4, 235-242, 1980.
26. **H.J. Zimmermann**, *Fuzzy Set Theory and its Applications*, 2nd Edition, Kluwer Academic Publishers, Dordrecht, The Netherlands, 1991.
27. **H.T. Nguyen**, *N.R. Prasad, C.L. Walker, E.A. Walker, A first course in Fuzzy and Neural Control*, Chapman & Hall/CRC, 2003
28. **Y. Dote**, *Introduction to Fuzzy Logic, Industrial Electronics, Control, and Instrumentation*, Orlando, 50-56, November 1995

A NEW FINITE ELEMENT METHOD DISCRETIZATION BASED ON DUAL FORMULATION OF MAGNETOSTATIC FIELD

Liviu **NEAMT**, Emil **MICU**
North University of Baia Mare, liviu.neamt@ubm.ro

Key words: Finite Element Method, Meshing, Magnetostatic field
Abstract: The meshing techniques are very important for the economy and the precision of a Finite Eelment Method (FEM) analysis. The presented algorithm for the discretization of a magnetostatic plane parallel configuration is based on dual formulation of magnetostatic field and generates, in iterative steps, a final mesh which is very close to the magnetostatic spectrum, magnetic field lines and equipotentials lines for scalar magnetic potential.

1. INTRODUCTION

Discretization of the problem region is the most delicate step, the bigger error generator of an FEM field analysis. Using triangular first order elements, with a careful meshing, the solutions have good accuracy and the mathematical problem becomes simple. Generated particularities, offering the solution as joined uniform fields with fixed geometrical position established in preprocessor by discretization, rarely gives an acceptable ratio: accuracy, number of nodes. So the mesh refinement techniques, permanently adapted to the level of error, are a compulsory step in modern FEM. Proposed algorithm goes to obtain the best solution with the initially imposed number of nodes without increasing the polynomial order of elements. Also it offers the possibilities to reduce the studied domain and to improve the domain frontiers and/or the associated conditions if there are imposed using truncation methods [3]. Dual formulations of the magnetostatic fields generate simplicity, a very strong error estimator, not needing numbering techniques and composing the system matrix, etc.

2. DUAL FORMULATION OF MAGNETOSTATIC FIELDS

In current-free regions magnetostatic simulation implies simultaneously solving the equations,

$$\nabla \overline{B} = 0 \tag{1}$$

$$\nabla \times \overline{H} = 0 \tag{2}$$

$$\overline{B} = \mu_0 \mu_r (H) \cdot \overline{H} \tag{3}$$

associated with boundary conditions at the interface Γ between media 1 and media 2,

$$\overline{n} \times \left(\overline{H_1} - \overline{H_2} \right)\Big|_{\Gamma} = 0 \tag{4}$$

$$\overline{n} \cdot (\overline{B_1} - \overline{B_2})\Big|_{\Gamma} = 0 \tag{5}$$

Introducing both magnetic potentials, vector and scalar,

$$\overline{B} = rot\,\overline{A} \tag{6}$$

$$\overline{H} = -\nabla V_m \tag{7}$$

two mathematical formulations are available:

- Electrical where (1), (3), (5) are verified exactly, the errors are in (2), (4) that is magnetic vector potential formulation,
- Magnetical where (2), (3), (4) are verified exactly, the errors are in (1), (5) that is magnetic scalar potential formulation.

3. FEED BACK CRITERIA

The success of a mesh adaption algorithm is strongly dependent on the feed back criteria. Starting from the dual formulation of the magnetostatic fields it is easy to estimate the error of the analysis using error in constitutive relation [2] that has the main advantage to be the upper bound of the exact error. With $\overline{B}$ and $\overline{H'}$, the FEM solutions obtained from vector, respectively scalar magnetic potentials,

$$e = \overline{B} - \mu \overline{H'} \tag{10}$$

The global absolute and relative error associated are defined in a bounded domain D,

$$e_{abs}^2 = \frac{1}{2} \int_D \frac{1}{\mu} \left(\overline{B} - \mu \overline{H'} \right)^2 dD \tag{11}$$

$$\varepsilon^2 = \frac{\int_D \frac{1}{\mu}\left(\overline{B} - \mu H'\right)^2 dD}{\int_D \frac{1}{\mu}\left(\overline{B} + \mu \overline{H'}\right)^2 dD} \tag{12}$$

4. SPECTRUM TYPE DISCRETIZATION

An imputed initial mesh, generator of the field geometry and the maximum number of nodes, start a typically dual FEM analysis. The solution of the potentials (vectorial and scalar) allows to calculate the position of intersections between flux lines and equipotentials, solving the equations system:

$$\begin{cases} V_{imp}(k_2) = a + b \cdot x(k_1, k_2) + c \cdot y(k_1, k_2) \\ A_{imp}(k_1) = a_1 + b_1 \cdot x(k_1, k_2) + c_1 \cdot y(k_1, k_2) \end{cases} \tag{13}$$

with V_{imp} and A_{imp} the scalar and vector potentials choused to generate the field spectrum and constants *a, b, c,* a_1, b_1, c_1 computed from the "old" coordinates of the nodes and corresponding values of the potentials:

$$\begin{pmatrix} a \\ b \\ c \end{pmatrix} = \begin{pmatrix} 1 & x_1 & y_1 \\ 1 & x_2 & y_2 \\ 1 & x_3 & y_3 \end{pmatrix}^{-1} \begin{pmatrix} V_{m1} \\ V_{m2} \\ V_{m3} \end{pmatrix} \tag{14}$$

Replacing V_m with *A,* we obtain the constants for vector potentials equations.

The cycle is repeated until the imposed error for geometrical displacement of the mesh is reached.

For the e element, see fig. 1.a, based on FEM calculation of the magnetic flux density and field:

$$gradA = \bar{i}\frac{\partial A}{\partial x} + \bar{j}\frac{\partial A}{\partial y} = \frac{1}{2S}\left[(y_3 - y_2)\bar{i} - (x_3 - x_2)\bar{j}\right](A_2 - A_1) \tag{15}$$

$$gradV_m = \bar{i}\frac{\partial V_m}{\partial x} + \bar{j}\frac{\partial V_m}{\partial y} = \frac{1}{2S}\left[(y_3 - y_1)\bar{i} - (x_3 - x_1)\bar{j}\right](V_{m2} - V_{m1}) \tag{16}$$

$$\overline{H'} = \frac{1}{2S}\left[-(y_3 - y_1)\bar{i} + (x_3 - x_1)\bar{j}\right](V_{m2} - V_{m1}) = \frac{1}{2S}(V_{m2} - V_{m1})l_{13}\overline{n_{13}} \tag{17}$$

$$\overline{B} = -\frac{1}{2S}\left[(x_3 - x_2)\bar{i} + (y_3 - y_2)\bar{j}\right](A_2 - A_1) = \frac{1}{2S}(A_2 - A_1)\bar{l}_{32} \tag{18}$$

with simple geometrical calculation it is easy to see that the interelemental boundary conditions are satisfied with the position precision.

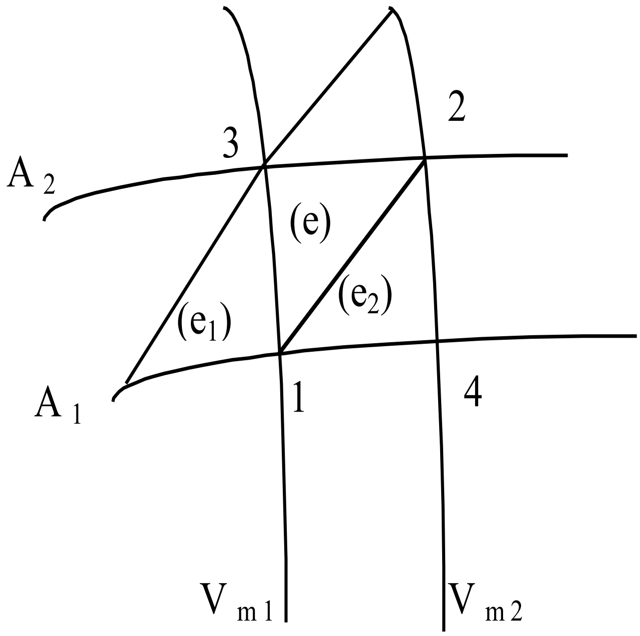

Fig.1. a. An element of the spectrum type discretization

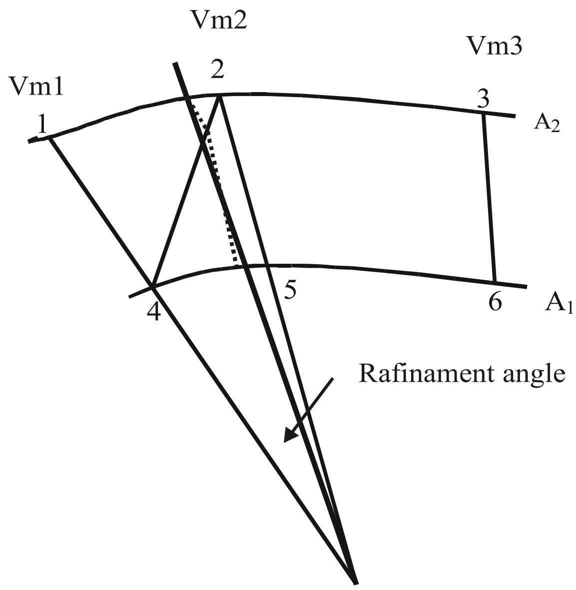

Fig.1. b. Refinement of the equipotential line 25

The feed back criteria, for each element, is reached if the error in constitutive relation become scalar and:

$$e_{(e)} = B - \mu H' = \frac{1}{2S}\left(l_{23}\left|A_2 - A_1\right| - \mu l_{13}\left|V_{m_2} - V_{m_1}\right|\right) = 0 \text{ or } \frac{l_{23}}{l_{13}} = \mu\left|\frac{V_{m_2} - V_{m_1}}{A_2 - A_1}\right| \quad (19)$$

Satisfying both conditions goes to rectangular spectrum cells. With exception of the uniform field the zero error could not be touched.

The presented algorithm improved the analysis precision by transforming the spectrum cells in “most appropriate rectangles” choosing the best values of potentials V_{imp} and A_{imp}, given by the two refinement angles and two refinement directions.

The refinement directions have to be choused as the areas with most unaligned flux lines between two equipotentials and most unaligned equipotentials between two flux lines.

The calculus of the refinement angle is based on the determination of the arithmetical media of the same type of lines angles followed by the refinement directions. With these values there are computed the desired values to be imposed on potentials as shown in fig.1.b.. The position of line 25 is redrawn at the same angle to both neighborly lines 14, 36. The value for potential can belong to any point of intersection between the dotted line (FEM line in those two elements) and the frontiers. The last step of fitting the discretization trough the spectrum is recommended to validate the discretization.

A control of the boundary conditions becomes possible passing the quality of being the frontier to a close line of the spectrum. Choosing the new frontier as a far distance line or infinitely close one the analysis area will be decrease or not.

The entire algorithm computing schemes are based on recursive strategies given by the first impute of the mesh, made in a matrix disposal of nodes as intersections of equipotentials and flux lines. No numbering technique is necessary and the system matrix is not defined.

5. EXAMPLE

An infinite ferromagnetic (infinite relative magnetic permeability) wire is placed in a uniform magnetic field perpendicular to its filed lines. An initial 2162 nodes mesh, fig. 3.b, sets the geometry, fig.3.a.

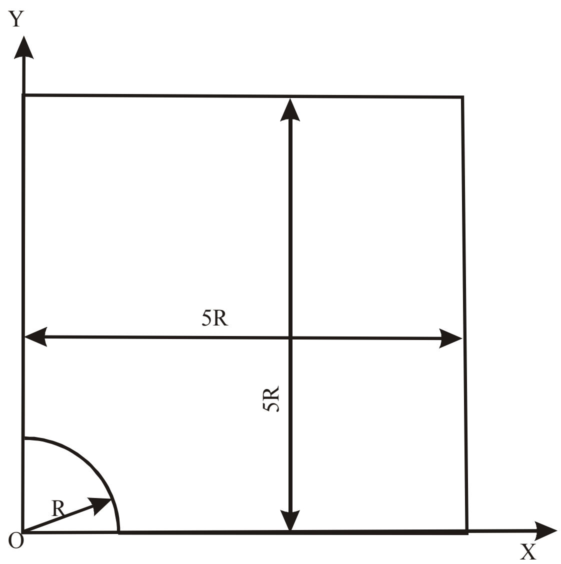

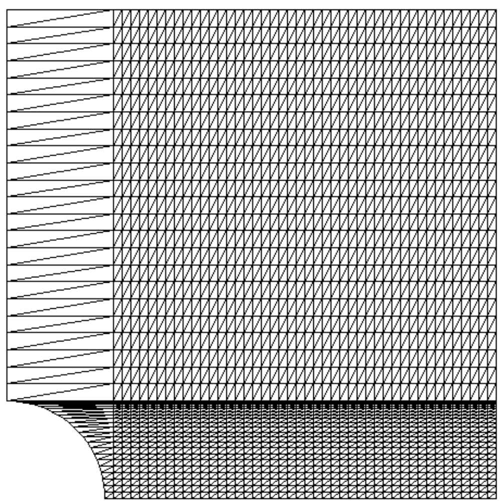

Fig.3.a. The geometry of the analysis domain; b. The 2162 initial mesh

The refined mesh, witch also performed the decreasing of the analysis domain to a quarter of started one, shown in Fig. 4.a, generate the magnetic spectrum, Fig.4.b and reached the global relative error 1.53% in tree steps.

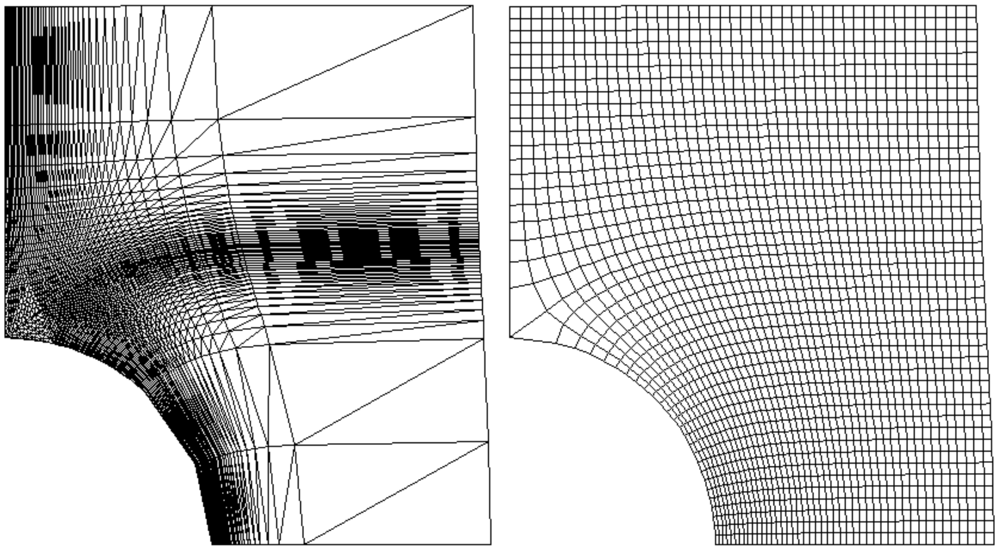

Fig.4. a. Refined mesh; b. magnetic spectrum

REFERENCES

1. Fee J, Dyczij E.R. *Application of steepest descendent smoothing and de-meshing techniques in H-version adaptive FEMs*, IEEE Trans. on magnetics, vol 35, nr.3, may 1999

2. Remacle J, Dular P. *A posteriori error estimation and adaptive meshing using error in constitutive relation*, IEEE Trans. on magnetics, vol 32, nr.3, may 1996

3. Chen Q, Konrad A. *A review of finite element open boundary techniques for static and quasistatic electromagnetic field problems,* IEEE Trans. on magnetics, vol 33, nr.1, Jan 1997

4. **Taylor S, Sykulski J.K**. *Anisotropic adaptive mesh refinement for electromagnetics Fea in 2D*, IEEE Trans. on magnetics, vol 35, nr.3, may 1999

INSTRUCTIONS FOR AUTHORS

Name **SURNAME**, Name **SURNAME, ...**

Affiliation, email of 1st author, Affiliation, email of 2nd author, ...

Key words: List 3-4 keywords

Abstract: *Abstract of max. 120 words*

1. INTRODUCTION

The paper must be written in English. It shall contain at least the following chapters: Introduction, research course (mathematical algorithm); method used; results and conclusions, references.

Use DIN A4 Format (297 x 210 mm) MSWord format. Margins: top, bottom, left and right 2.5 mm each. The text should be written on one side of the page only. Use Times New Roman fonts, line spacing 1.3. The font formats are: paper title: 14 pt bold italic, capital letters, author's name(s): 12 pt italic for name and 12 pt. bold, italic for surname; Affiliation: 11 pt. italic; key words: 10 pt, bold; Abstract: 10 pt. italic, word Abstract in 10 pt. bold; chapter titles (do not use automatic numbering): 12 pt bold, capital letters; subtitles: 12 pt bold lower capitals; body text: 12 pt. regular. tables and figures caption: 11 pt. italic; references: author 11 pt. bold, title 11 pt. italic, year, pages, ... in regular.

The number of pages is not restricted.

2. FIGURES AND TABLES

Figures have to be made in high quality, which is suitable for reproduction and print. Don't include photos or color prints. Place figures and tables at the top or bottom of a page wherever possible, as close as possible to the first reference to them in the paper.

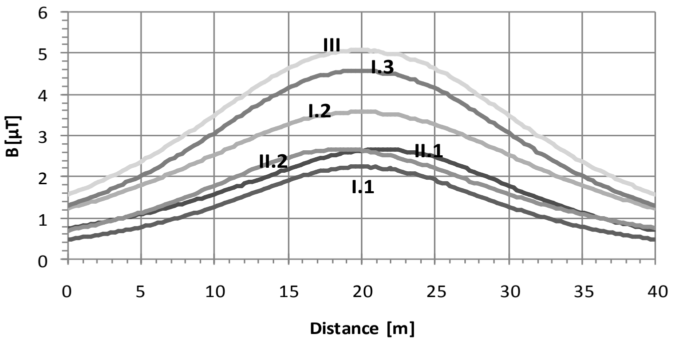

Fig. 4 - Magnetic flux density at 1 m above the ground

Table1. Transposing principle

	Circuit											
	1	*2*	*1*	*2*	*1*	*2*	*1*	*2*	*1*	*2*	***1***	***2***
1/3	*R*	*T*	***R***	***R***	*R*	*S*	*R*	*T*	*R*	*S*	***R***	***R***
line	***S***	***S***	*S*	*T*	*S*	*R*	*S*	*R*	*S*	*T*	***S***	***S***
length	*T*	*R*	*T*	*S*	***T***	***T***	*T*	*S*	*T*	*R*	***T***	***T***
1/3	*T*	*S*	***T***	***T***	*T*	*R*	*T*	*S*	*T*	*R*	***T***	***T***
line	***R***	***R***	*R*	*S*	*R*	*T*	*R*	*T*	*R*	*S*	***R***	***R***
length	*S*	*T*	*S*	*R*	***S***	***S***	*S*	*R*	*S*	*T*	***S***	***S***
1/3	*S*	*R*	***S***	***S***	*S*	*T*	*S*	*R*	*S*	*T*	***S***	***S***
line	***T***	***T***	*T*	*S*	*T*	*S*	*T*	*S*	*T*	*R*	***T***	***T***
length	*R*	*S*	*R*	*T*	***R***	***R***	*R*	*T*	*R*	*S*	***R***	***R***
Name	***I.1***		***I.2***		***I.3***		***II.1***		***II.2***		***III***	

3. EQUATIONS

Equations are centred on page and are numbered in round parentheses, flush to right margin. In text respect the following rules: all variables are italic, constants are regular; the references are cited in the text between right parentheses: [1], the list of references has to be arranged in order of citation.

REFERENCES

1. International Commission on Non-ionizing Radiation Protection, *Guidelines for limiting exposure to time-varying electric, magnetic and electromagnetic fields (Up to 300 GHz)*, Health Physics, **74**, pp. 494-522, 1998.

2. A. Marincu, M. Greconici, *The electromagnetic field around a high voltage 110 KV electrical overhead lines and the influence on the biological sistems,* Proceedings of the 5th International Power Systems Conference, pp. 357-362, Timisoara, 2003.

3. Gh. Hortopan, *Compatibilitate electromagnetică,* Ed. Tehnică, 2005.